Published in final edited form as:
Life Sci. 2021 November 01; 284: 119845. doi:10.1016/j.lfs.2021.119845.

Acute gene expression changes in the mouse hippocampus following a combined Gulf War toxicant exposure

Kathleen E. Murray[a,c,1], **Vedad Delic**[a,c,e,2], **Whitney A. Ratliff**[d,3], **Kevin D. Beck**[b,c,e,4], **Bruce A. Citron**[a,c,d,e,*,2]

[a]Laboratory of Molecular Biology, VA New Jersey Health Care System, Research & Development (Mailstop 15), Bldg. 16, Rm. 16-176, 385 Tremont Ave, East Orange, NJ 07018, United States of America

[b]Neurobehavior Research Laboratory, VA New Jersey Health Care System, Research & Development (Mailstop 15), Bldg. 16, Rm. 16-176, 385 Tremont Ave, East Orange, NJ 07018, United States of America

[c]Rutgers School of Graduate Studies, Newark, NJ 07103, United States of America

[d]Laboratory of Molecular Biology, Bay Pines VA Healthcare System, Research and Development, 151, Bldg. 22, Rm. 123, 10000 Bay Pines Blvd, Bay Pines, FL 33744, United States of America

[e]Pharmacology, Physiology, and Neuroscience, Rutgers-New Jersey Medical School, Newark, NJ 07103, United States of America

Abstract

Aims: Approximately 30% of the nearly 700,000 Veterans who were deployed to the Gulf War from 1990 to 1991 have reported experiencing a variety of symptoms including difficulties with learning and memory, depression and anxiety, and increased incidence of neurodegenerative diseases. Combined toxicant exposure to acetylcholinesterase (AChE) inhibitors has been studied extensively as a likely risk factor. In this study, we modeled Gulf War exposure in male C57Bl/6J mice with simultaneous administration of three chemicals implicated as exposure hazards for Gulf War Veterans: pyridostigmine bromide, the anti-sarin prophylactic; chlorpyrifos, an organophosphate insecticide; and the repellant *N,N*-diethyl-*m*-toluamide (DEET).

Main methods: Following two weeks of daily exposure, we examined changes in gene expression by whole transcriptome sequencing (RNA-Seq) with hippocampal isolates.

[*]Corresponding author at: VA New Jersey Health Care System, Laboratory of Molecular Biology, Research and Development, Building 16, Room 16-176, 385 Tremont Ave., East Orange, NJ 07018, United States of America. bruce.citron@rutgers.edu (B.A. Citron).
[1]Laboratory of Molecular Biology, Research and Development, Building 1, Room 9-169, 385 Tremont Ave., East Orange, NJ 07018.
[2]Laboratory of Molecular Biology, Research and Development, Building 16, Room 16-176, 385 Tremont Ave., East Orange, NJ 07018.
[3]10000 Bay Pines Blvd., Bay Pines VA Healthcare System, Laboratory of Molecular Biology, Research and Development 151, Bldg. 22, Rm. 123 R&D 151, Bay Pines, FL 33744-4125.
[4]Neurobehavior Research Laboratory, Research and Development, Building 16, Room 16-184, 385 Tremont Ave., East Orange, NJ 07018.

Declaration of competing interest

No competing financial interests exist. The contents do not represent the views of the Department of Veterans Affairs or the United States Government, and the opinions, interpretations, conclusions and recommendations are those of the authors and are not necessarily endorsed by the Department of Defense.

Hippocampal-associated spatial memory was assessed with a Y-maze task. We hypothesized that genes important for neuronal health become dysregulated by toxicant-induced damage and that these detrimental inflammatory gene expression profiles could lead to chronic neurodegeneration.

Key findings: We found dysregulation of genes indicating a pro-inflammatory response and downregulation of genes associated with neuronal health and several important immediate early genes (IEGs), including *Arc* and *Egr1*, which were both reduced approximately 1.5-fold. Mice exposed to PB + CPF + DEET displayed a 1.6-fold reduction in preference for the novel arm, indicating impaired spatial memory.

Significance: Differentially expressed genes observed at an acute timepoint may provide insight into the pathophysiology of Gulf War Illness and further explanations for chronic neurodegeneration after toxicant exposure.

Keywords

Gulf War; RNA-Seq; Gene expression; Pyridostigmine bromide; Chlorpyrifos; DEET; Arc; Immediate early genes; Hippocampus

1. Introduction

Gulf War Illness (GWI) is a chronic multi-system disorder affecting approximately 30% of Veterans deployed during Operations Desert Shield and Desert Storm from August 1990 to February 1991 [1–5]. GWI encompasses a wide spectrum of symptoms which typically include some combination of fatigue/sleep problems, pain, neurological/mood/cognitive impairments, respiratory complaints, gastrointestinal problems, or skin symptoms [6,7]. Of particular interest are neurocognitive impairments and effects on the central nervous system (CNS), as Gulf War Veterans have significantly higher rates of neurological disorders, including amyotrophic lateral sclerosis (ALS), brain cancers, stroke, migraines, neuritis, and neuralgia, than other veteran populations [7]. Research findings in Gulf War animal models have demonstrated that a wide array of physiological alterations including changes in behavior, cognition, neurotransmission, axonal transport, genomic, proteomic, lipidomic, and metabolomic profiling, and mitochondrial dysfunction result from Gulf War exposure [1–5,7,8].

Military personnel deployed during the Gulf War were exposed to an array of chemical exposures in tandem, particularly acetylcholinesterase (AChE) inhibitors. Investigations into the effects of combined Gulf War exposures vary widely but typically include some combination of insecticides, insect repellants, nerve agents, and anti-toxins against nerve agents [1–3,7]. Our Gulf War toxicant mixture includes chemicals from three of the most frequently investigated of these classes: specifically, pyridostigmine bromide (PB, a reversible AChE inhibitor administered as a sarin prophylactic), chlorpyrifos (CPF, an organophosphate pesticide), and *N*,*N*-diethyl-*m*-toluamide (DEET, a common insect repellent).

Significant pathological changes in the hippocampus and corresponding impairments in hippocampal-dependent learning and memory have been observed in several animal models of Gulf War toxicant exposure. Rats exposed to low doses of DEET, permethrin, PB, and

restraint stress for four weeks showed significantly reduced hippocampal volume and neuron growth as well as increased occurrence of activated microglia and astrocyte hypertrophy which was accompanied by spatial learning and memory dysfunction [9]. The combination of PB and DEET has been shown to influence cholinesterase activity in the rodent brain and affect seizures [10,11]. Organophosphate exposure has also been shown to impair spatial navigation learning in the Morris Water Maze task [12,13]. Neurotoxicity following administration of PB + CPF + DEET was originally reported by Abou-Donia et al. in hens exposed to 5 mg/kg PB i.o., 10 mg/kg CPF s.c., and 500 mg/kg DEET s.c. 5 days/week for 2 months [14]. Ojo et al. reported significant pathological changes in the hippocampus and cortex of C57Bl/6 mice exposed to PB + CPF + permethrin at an acute timepoint (72 h post-exposure) [15].

Transcriptional changes after Gulf War toxicant exposure in rodent models have mostly focused on epigenetic changes or investigation of specific gene categories of interest at chronic timepoints [8,16–19]. We assessed acute changes in gene expression in mouse hippocampal RNA isolates after exposure to a combined subcutaneous (s.c.) injection of PB, CPF, and DEET for two weeks using whole transcriptome sequencing (RNA-Seq). We focused on genes important for neuronal health, those that could affected by toxicants, and those involved in inflammatory responses. Differentially expressed genes observed at an acute timepoint may set the stage for chronic outcomes and should provide insight into the pathophysiology of Gulf War Illness and help identify potential targets for future treatment.

2. Materials and methods

2.1. Chemicals

HPLC-grade pyridostigmine bromide (PB, P9797) and *N,N*-diethyl-*m*-toluamide (DEET, D100951) were obtained from Sigma-Aldrich (St. Louis, MO). Chlorpyrifos (CPF, N-11459) was obtained from Chem-Service, Inc. (West Chester, PA). The toxicant mixture stock was prepared and stored in 500 μL aliquots at −20 °C until use and diluted in PBS immediately prior to injection. Vehicle for injection contained 3.125% dimethyl sulfoxide (DMSO, 99.9%, D2438-5X10ML) obtained from Thermo Fisher Scientific (Waltham, MA) in 1x PBS.

2.2. Subjects

All animal experiments were performed in accordance with the guidelines of the institution, the National Institutes of Health guide for the Care and Use of Laboratory Animals and approved by the East Orange VA and Bay Pines VA Institutional Animal Care and Use Committees. Animals were single-housed in a 22 °C ± 0.5 °C temperature-controlled environment with a 12-hour light/dark cycle. Animals were allowed a 7-day acclimation period before switching to a reverse light cycle (i.e., dark cycle from 10 am-10 pm) for 5 days prior to exposure. Food and water were available ad libitum throughout for all animals.

2.3. Toxicant exposure

Male C57Bl/6 J mice were obtained from Charles River (Wilmington, MA) for RNA-Seq (n = 6/group) and from Jackson Laboratory (Bar Harbor, ME) for behavior (n = 6/group) based

on availability. Mice received daily s.c. injections of either the toxicant mixture containing 2.5 mg/kg PB, 12.5 mg/kg CPF, and 7.5 mg/kg DEET with 3.125% DMSO in PBS or vehicle containing 3.125% DMSO in PBS five days a week (M-F) for two weeks beginning at 12 weeks of age. Adverse effects including seizures resulting in removal and euthanasia, were observed at 1.5- and 2.0-fold higher dosages, but this was extremely rare at the dosage used in this study. Experimental cohorts which generated RNA-seq and behavioral data did not display any significant adverse effects. For RNA-Seq, mice were sacrificed 2–4 h after the final exposure via cervical dislocation and decapitation. Whole brains were immediately extracted, and hippocampal tissue from each hemisphere was dissected and snap frozen on dry ice. All fresh frozen tissue samples were stored at −70 °C until use.

2.4. Y-maze task with preference index

To assess hippocampal-dependent memory, subjects underwent a modified Y-maze task 2–4 h after the final exposure. During the training phase, either Arm B or C (novel arm) was blocked off with a barrier. The novel arm was randomly assigned for each trial. Mice were placed in the start arm (Arm A) of the Y-maze facing the wall and allowed to explore the start and familiar arms for 8 min. Mice were then removed from the maze and returned to their home cage for an intertrial interval of 30 min. During the trial phase, the barrier was removed so that all three arms were accessible. Mice were again placed in the start arm and allowed to explore the start and familiar arms for 8 min. Behavior was captured with a video camera (DMK 22AUC03, The Imaging Source, Charlotte, NC) and recorded by ANY-maze (version 6.17, Stoelting, Wood Dale, IL). Time or entry into a zone was scored based on the center point of the animal's body. All Y-maze trials were performed under red light during the dark cycle.

2.5. RNA isolation

Hippocampal RNA was isolated by TRIzol (Invitrogen, Waltham, MA) extraction followed by cleanup with a RNeasy Mini Kit (QIAGEN, Hilden, Germany). Tissue was resuspended in 0.4 mL TRIzol and homogenized with a Polytron homogenizer (Kinematica USA, Bohemia, NY) on ice for 30–45 s. Samples were incubated at 23 °C for 5 min before adding 80 μL $CHCl_3$ and vortexing for 15 s. Samples were incubated at 23 °C again for 2–3 min. Tubes were centrifuged at 12,000 rcf for 10 min, and the supernatant was transferred into a new tube with an equal volume of 70% EtOH. RNeasy Mini Kit was then used per the manufacturer's instructions with Tris-EDTA buffer (TE, pH 8.0, AM9858, Invitrogen) for the final elution step. All RNA isolates were stored at −20 °C until use.

2.6. RNA-Seq

RNA isolates were sequenced by the Rutgers-New Jersey Medical School Genomics Center. Total cellular RNA was qualified by confirming integrity with a 2200 TapeStation (Agilent Technologies, Santa Clara, CA). Samples with an RNA integrity number (RIN) > 7.0 were used for subsequent processing. Total RNAs were subjected to two rounds of poly (A) selection using Oligo $d(T)_{25}$ Magnetic Beads (New England Biolabs, Ipswich, MA). RNA-Seq libraries were prepared using an NEBNext Ultra RNA Library Prep Kit for Illumina (New England Biolabs). cDNA libraries were purified with AMPure XP beads (Beckman Coulter, Brea, CA) and quantified using a Qubit 4 Fluorometer (Thermo Fisher Scientific).

Equimolar amounts of barcoded libraries were pooled and sequenced on a NextSeq 500 Sequencing System (Illumina, San Diego, CA) with a 1 × 75 configuration.

2.7. RNA-Seq analysis

RNA-Seq reads were imported into CLC Genomics Workbench (version 20.0.3, QIAGEN) for preliminary analysis using a modified version of the workflow for RNA-Seq analysis with export to IPA (Fig. 1). All reads were batch processed and mapped to the *Mus musculus* reference genome. Control vs. PB + CPF + DEET samples were quantified using the Differential Analysis for RNA-Seq tool. Differentially expressed genes were considered significant if they met the following criteria: mean reads per kilobase of transcript per million mapped reads (RPKM) > 10.0, fold change in either direction ≥1.2, and $p < 0.1$. Gene ontology (GO) categories were assigned and analyzed for significance for biological processes, molecular functions, and cellular components using the Gene Set Test tool. GO categories were considered significant if fold change in either direction ≥1.2 and $p < 0.05$. Significant genes were exported to IPA.

Functional analyses were generated using Ingenuity Pathway Analysis (IPA) (QIAGEN). Core analysis was performed on dataset based on RPKM values for genes that met criteria for significance, which generated lists of significant canonical pathways, upstream regulators, associated diseases and functions, and differentially expressed genes. Canonical pathways were based on significant differentially expressed genes, and a pathway itself was considered significant if $p < 0.05$.

2.8. Statistics

All statistical analyses for behavior were conducted using GraphPad Prism for macOS (version 9.0.0). Mean values for behavioral analyses are depicted ± standard error of the mean (SEM). Data for open field and Y-maze tasks were analyzed using an unpaired *t*-test with Welch's correction, and statistical significance was considered when $p < 0.05$. Entries into each arm during the Y-maze task were analyzed using multiple unpaired *t*-tests followed by FDR control with the two-stage step-up method of Benjamini, Krieger, and Yekutieli as recommended by GraphPad. Significant fold changes in RNA expression were analyzed by CLC Genomics Workbench using Differential Expression for RNA-Seq as part of the workflow as detailed in Fig. 1.

3. Results

3.1. Effects of Gulf War toxicant exposure on hippocampal-dependent spatial memory in Y-maze task

To assess effects of the exposure on hippocampal-dependent spatial memory, mice underwent a Y-maze task ($n = 6$/group). Time spent in each arm, number of entries into each arm, and distance travelled were recorded. Preference for the novel arm was significantly lower by 157% in mice exposed to PB + CPF + DEET compared to controls, $p = 0.027$ (Fig. 2a). The number of entries into the novel arm was also significantly reduced by 33% compared to control mice, $p = 0.003$ (Fig. 2b). Distance travelled during the test stage

was only 12% lower in toxicant-exposed mice compared to controls and therefore did not significantly differ between conditions, $p = 0.182$ (Fig. 2c).

3.2. Gene dysregulation after acute exposure to Gulf War toxicants

In the hippocampus, 158 dysregulated genes were identified with the aid of RNA-Seq analysis which met criteria for differential expression in response to Gulf War toxicant exposure (Fig. 3, Tables 1 and 2). A gene set test (GO enrichment analysis) in CLC Genomics Workbench showed significantly affected gene ontology (GO) categories. Of these categories, 47 were related to biological processes (Table 4a), 138 were related to molecular functions (Table 4b), and 120 were related to cellular components (Table 4c). Pathway analysis in IPA showed 45 significantly affected canonical pathways (Table 3).

The most significantly affected canonical pathways after exposure included protein ubiquitination (*B2m*, *Dnaja1*, *Dnajb4*, *Hba-a2*, *Hsp90aa1*, *Hsp90b1*, *Hspa4l*, *Hspa5*, *Ube2q2*), aldosterone signaling in epithelial cells (*Dnaja1*, *Dnajb4*, *Hsp90aa1*, *Hsp90b1*, *Hspa4l*, *Hspa5*, *Plcb1*), hypoxia signaling in the cardiovascular system (*Hsp90aa1*, *Hsp90b1*, *Nfkbia*, *Pten*, *Ube2q2*), unfolded protein response (*Hsp90b1*, *Hspa5*, *Srebf1*), endoplasmic reticulum (ER) stress pathway (*Hsp90b1*, *Hspa5*), and the neuroinflammation signaling pathway (*B2m*, *Gabra2*, *Gabrb1*, *Gad2*, *Hba-a2*).

We observed dysregulation of genes indicative of a pro-inflammatory response, including downregulation of *B2m* and *Hba-a2* and upregulation of *Gabra2*, *Gabrb1*, and *Gad*. There was significant downregulation of several genes associated with neuronal health, particularly genes involved in the integrity of the myelin sheath (*Mog*, *Mbp*, *Mag*, *Pllp*, *Pmp22*, *Cldn11*, *Cnp*), neurogenesis (*Arc*, *Opalin*), dendritic cell maturation (*B2m*, *Hba-a2*), NF-κB inhibition (*Nfkbia*, *Plcb1*), and learning and memory (*Arc*). Additionally, we found significant downregulation of mitochondrial genes coding for the F0 subunit of the proton-transporting ATP-synthase complex (*mt-Atp6*, *mt-Atp8*). There was significant upregulation of pro-apoptotic genes (*Pten*), genes involved in ER stress response (*Hspa5*, *Hsp90b1*), and genes involved in organonitrogen compound metabolism (*Lars2*, *Hmgn5*). There was also upregulation of genes implicated in related neurodegenerative diseases, including *Oxr1*, *Top1*, and *Cdr1*.

We observed dysregulation in GO categories of interest relating to biological processes, molecular functions, and cellular components. Significantly affected biological processes included leucyl-tRNA aminoacylation (*Lars2*), regulation of neurogenesis (*Arc*, *Opalin*), peptide metabolic process (*Hmgn5*, *Lars2*), regulation of long-term synaptic depression (*Arc*), regulation of postsynaptic neurotransmitter receptor internalization (*Arc*), and mitochondrial translation (*Lars2*). Notably affected GO categories involved in molecular functions included RNA strand annealing activity (*Fmr1*, *Fxr1*), supercoiled DNA binding (*Psip1*, *Top1*), and unfolded protein binding (*Dnajb4*, *Hsp90aa1*, *Hsp90b1*, *Hspa5*). Significantly affected GO categories forming cellular components of interest included the myelin sheath (*Cldn11*, *Cnp*, *Dld*, *Gjc2*, *Gsn*, *Hsp90aa1*, *Hspa5*, *Mag*, *Mbp*, *Mog*, *Plcb1*, *Sucla2*), GABAergic synapses (*Camk4*, *Cnr1*, *Gabra2*, *Gabrb1*, *Gabrd*, *Nrxn1*, *Plcb1*, *Slc6a6*), dendritic spines (*Akap5*, *Arc*, *Fmr1*, *Fxr1*, *Homer1*, *Lpar1*, *Mob4*, *Pten*, *Slc8a1*, *Syndig1*), ER chaperone complex (*Hsp90b1*, *Hspa5*, *Sdf2l1*), MHC class I peptide loading

complex (*B2m*, *H2-D1*, *H2-K1*), and endocytic vesicles (*Gsn*, *Kif5b*, *Lpar1*, *Nrxn1*, *Rab8b*, *Rab9b*, *Rabep1*, *Trf*), among others.

4. Discussion

Our results showed that subcutaneous administration of PB + CPF + DEET for two weeks induced acute changes in gene expression in mouse hippocampal tissue, including dysregulation of genes indicating a pro-inflammatory response, downregulation of genes associated with neuronal health, and upregulation of pro-apoptotic genes, genes involved in ER stress response, and genes implicated in neurogenerative diseases, among others. We also observed significant effects of our Gulf War exposure on spatial memory.

The three most significantly downregulated genes after exposure were *Arc*, *Egr1*, and *Nr4a1*, all of which are neuronal immediate early genes (IEGs). Arc is predominantly expressed in cortical and hippocampal glutamatergic neurons and is involved in numerous neuronal signaling pathways [20,21]. *Arc* knockout mice display deficits in long-term memory formation in implicit and explicit learning tasks and impaired long-term potentiation (LTP) and depression (LTD) [22]; similar effects on LTP and spatial learning were shown in rats after chemical inhibition of *Arc* [23]. *Egr1* is required for stabilization of synaptic plasticity in the hippocampus as well as formation of both hippocampal and non-hippocampal-dependent long-term memory [24] and is a direct transcriptional regulator of *Arc* [25].

Although IEGs are classified as such due to their early and transient response to environmental stimuli, both *Arc* and *Egr1* also play critical roles in mediating the structural changes that underlie neuronal and synaptic plasticity, suggesting that their dysregulation could trigger long-term morphological changes with negative impacts on learning and memory formation. Several mouse models of Alzheimer's disease (AD) report early dysregulation of IEGs involved in LTP and synaptic plasticity [26]. Dickey et al. observed a significant decrease in basal *Arc*, *Egr1*, and *Nr4a1* expression in amyloid-containing hippocampus and cortex of APP/PS1 transgenic mice [27]. Levels of basal and exploration-induced *Arc* expression are significantly reduced in granule cells of the dentate gyrus of $hAPP_{FAD}$ transgenic mice [28]. Induced *Arc* expression was also dysregulated in the CA3 region and dentate gyrus of rats chronically infused with lipopolysaccharide (LPS) to induce neuroinflammation, suggesting altered patterns of *Arc* expression may contribute to cognitive and memory impairments in neurodegeneration [29]. IEGs have been investigated as a potential therapeutic target in AD treatment [30,31].

IEGs such as *Arc* and *Egr1* have also been suggested to play a critical role in the interaction between genes and environment to determine the risk of developing psychiatric illness, particularly major depressive disorder (MDD), which is typically comorbid with GWI [1–7,32–35]. Chronic treatment with various antidepressants targeting serotonin and norepinephrine can also restore *Arc* expression in the hippocampus and prefrontal cortex [36,37].

Additionally, *Arc* inhibits the binding of heat shock factor 1 (HSF1) to the heat shock element (HSE) in heat shock protein (HSP) gene promoters and prevents activation of

HSP genes [38]. Accordingly, we observed upregulation of Hsp genes, including Hsp40s (*Dnajb4*, *Dnaja1*), Hsp70s (*Hspa4l*, *Hspa5*), and Hsp90s (*Hsap90aa1*, *Hsp90b1*) and found that these genes were involved in several significantly affected pathways, including protein ubiquitination, aldosterone signaling, hypoxia signaling, unfolded protein response, interferon induction and antiviral response, and the ER stress pathway, among others. Thus, dysregulation of IEGs may play a role in acute neuroinflammation, leading to chronic neurodegeneration.

Interestingly, several genes encoding proteins that are structural components of myelin were downregulated, including *Mbp*, *Mag*, *Mog*, and *Cnp*. Myelin basic protein (Mbp) is phosphorylated by MAP kinase in response to action potential firing during LTP in the hippocampus [39,40]. Plasma autoantibodies against Mbp have also been found to be significantly increased in Veterans with symptoms of GWI compared to healthy controls [41,42]. We also observed dysregulation of genes related to the GABAergic synapse, including *Camk4*, *Cnr1*, *Gabra2*, *Gabrb1*, *Gabrd*, *Nrxn1*, *Plcb1*, and *Slc6a6*. Chronically, decreased GABA has been reported in hippocampi of mice exposed to PB + permethrin + DEET three months after exposure [43]. Additionally, we found decreased expression of *Chrm3*, which codes for the M_3 muscarinic receptor. Decreased M_3 receptor density has been reported in the CA1 region, CA3 region, and molecular layer of the hippocampus in C57Bl/6 mice exposed to PB + stress [44]. This suggests that changes in $GABA_A$ and M_3 receptor expression may begin during the acute phase of chronic sublethal exposure to our Gulf War toxicants.

Reported dosages and routes of administration of Gulf War toxicants in rodent models have varied widely throughout the literature. The subcutaneous route of administration for exposure to PB + CPF + DEET has several advantages. PB was taken orally by military personnel and is frequently administered via gavage in animal models; however, PB has been shown to have poor bioavailability, suggesting that injection may deliver a more precise dosage [45]. There has also been a significant amount of investigation into the effects of stress in combination with PB and other toxicants, with results that indicate increased BBB permeability to toxicants in stressed animals [46]. Friedman et al. reported significant effects of PB + stress on levels of *c-Fos* and AChE mRNAs in mouse whole-brain homogenates, indicating that stress can be a confounding variable in gene expression data examining an early transcriptional response [47]. The subcutaneous route would not present potential stress from repeated oral gavage.

Subcutaneous administration also avoids variable absorption via dermal application of CPF and DEET, which would have been in contact with the skin of military personnel. A study by Keil et al. examining the immunotoxicology of DEET in female B6C3F1 mice elaborated on factors which are necessary to accurately compare exposures in animal models but are often not considered [48]. Many human and animal studies refer to dermal penetration rather than absorption into the bloodstream, which is not an equivalent measure due to the variability of absorption levels within and between species. Keil et al. reported that s.c. administration of 7.7 mg/kg/day DEET equates to an estimated mouse blood exposure level that encompasses estimated military exposure levels as well as estimated DEET usage by the general population. Additionally, Keil et al. argue that the emphasis placed on relevant

route of exposure in the literature has limited utility, particularly in the case of dermal exposures such as DEET or CPF. CPF, a lipophilic organophosphate, could accumulate within the brain to cause AChE inhibition at our acute timepoint, which could have an effect on behavioral outcomes. There are wide ranges of estimated absorption and metabolic rates between rodents and humans.

It should be noted that military personnel would have been exposed to these compounds at lower dosages, but this exposure occurred over longer periods of time. In rodent models, higher dosages are often used in a shorter time frame due to the lifespan of the animal and the window in which to study effects. Other studies have reported using similar dosages at these intervals: Lamproglou et al. reported i.o. administration of 1.5 mg/kg PB for 12 days (5 days on, 2 days off, 5 days on) in male Wistar rats [49]; Peden-Adams et al. treated female B6C3F1 mice treated with 15.5 mg/kg DEET, 2 mg/kg PB, and 500 mg/kg JP-8 s.c. for 14 days as a “low dose” group [50]; Torres-Altoro et al. reported treatment of female C57Bl/6 mice with 30 mg/kg CPF s.c. for 7 days, male FVB mice with 2.5 mg/kg PB + 5 mg/kg DEET s.c. for 15 days, and male C57Bl/6 treated with 1 mg/kg PB s.c. for 10 days [51]; and Mauck et al. treated male C57Bl/6 mice with 3 or 10 mg/kg PB for 7 days via s.c. ALZET pump [44]. These studies illustrate the similar range of concentrations over shorter time frames, as well as the potential advantages of s.c. administration for certain experiments.

Whole transcriptome sequencing has been used previously in several rodent models of Gulf War exposure. A similar study by Shetty et al. examined changes in gene expression using qRT-PCR after 4 weeks of exposure to PB + DEET + stress in male Sprague-Dawley rats; however, their samples, collected at a longer 6-month time point after the last exposure, presented a gene expression profile indicative of chronic neuroinflammation [16]. Gene expression profiles of GWI patients have also been studied to identify novel treatment strategies by examining the overlap of dysregulated genes with drug targets and in comparison with expression profiles of other diseases [52]. In contrast, our acute Gulf War exposure model shows early effects that do not appear in chronic exposure models, such as dysregulation of IEGs. Xu et al. also recently reported on acute transcriptional changes in BXD mouse strains after exposure to corticosterone + diisopropyl fluorophosphate (DFP) [19]. We believe that acute changes may prime chronic neurodegenerative processes; therefore, further research should investigate mechanistic connections between early responses to toxicant exposure and chronic symptoms, including memory deficits, mood disorders, and neurodegeneration.

5. Conclusion

This study provides an assessment of changes in gene expression in combined exposure to PB, CPF, and DEET and a unique gene expression profile at an acute timepoint. Many of the dysregulated genes involve inflammatory signaling and other pathways that are important for the health of neurons. The neurological effects of toxicants, including memory deficits, may begin soon after exposure, and future research will further define the way these responses increase with time due to aging and other influences.

Acknowledgments

We thank Julia A. Burton and Mihal Grinberg for their expert technical assistance and Joshua Karp, Shannon Clare, Elizabeth Chang, and Gabrielle Gallant for their input. We also thank the Rutgers-NJMS Genomics Center (Drs. Patricia Soteropoulos and Mainul Hoque) for RNA-Seq processing and advice. This study was supported by the Department of Veterans Affairs (Veterans Health Administration, Office of Research and Development, Rehabilitation Research and Development (I01RX001520 and IK2RX003253) and Biomedical Laboratory Research and Development (I21BX003514)), the Assistant Secretary of Defense for Health Affairs through the Congressionally Directed Gulf War Illness Research Program (W81XWH-16-1-0626), the War Related Illness and Injury Study Center (NJ), the Bay Pines Foundation, and the Veterans Bio-Medical Research Institute. The data discussed in this publication have been deposited in NCBI's Gene Expression Omnibus (Edgar et al., 2002) and are accessible through GEO Series accession number GSE180786 (https://www.ncbi.nlm.nih.gov/geo/query/acc.cgi?acc=GSE180786).

References

[1]. Institute of Medicine [IOM], Gulf War and Health: Volume 8: Update of Health Effects of Serving in the Gulf War, Washington, D.C, 2010.

[2]. Institute of Medicine [IOM], Chronic Multisymptom Illness in Gulf War Veterans: Case Definitions Reexamined, Washington, D.C, 2014.

[3]. United States Department of Veterans Affairs, Research Advisory Committee on Gulf War Veterans' Illnesses [RAC-GWI], Gulf War Illness and the Health of Gulf War Veterans: Scientific Findings and Recommendations, Washington, D.C, 2008.

[4]. Institute of Medicine [IOM], Gulf War Veterans: Treating Symptoms and Syndromes, Washington, D.C, 2001.

[5]. Institute of Medicine [IOM], Gulf War and Health: Treatment for Chronic Multisymptom Illness, Washington, D.C, 2013.

[6]. Steele L, Prevalence and patterns of gulf war illness in Kansas veterans: association of symptoms with characteristics of person, place, and time of military service, Am. J. Epidemiol 152 (2000) 992–1002, 10.1093/aje/152.10.992. [PubMed: 11092441]

[7]. White RF, Steele L, O'Callaghan JP, Sullivan K, Binns JH, Golomb BA, Bloom FE, Bunker JA, Crawford F, Graves JC, Hardie A, Klimas N, Knox M, Meggs WJ, Melling J, Philbert MA, Grashow R, Recent research on Gulf War illness and other health problems in veterans of the 1991 Gulf War: effects of toxicant exposures during deployment, Cortex 74 (2016) 449–475, 10.1016/j.cortex.2015.08.022. [PubMed: 26493934]

[8]. Dickey B, Madhu LN, Shetty AK, Gulf war illness: mechanisms underlying brain dysfunction and promising therapeutic strategies, Pharmacol. Ther 107716 (2020), 10.1016/j.pharmthera.2020.107716. [PubMed: 33164782]

[9]. Parihar VK, Hattiangady B, Shuai B, Shetty AK, Mood and memory deficits in a model of gulf war illness are linked with reduced neurogenesis, partial neuron loss, and mild inflammation in the hippocampus, Neuropsychopharmacology 38 (2013) 2348–2362, 10.1038/npp.2013.158. [PubMed: 23807240]

[10]. Chaney LA, Rockhold RW, Mozingo JR, Hume AS, Moss JI, Potentiation of pyridostigmine bromide toxicity in mice by selected adrenergic agents and caffeine, Vet. Hum. Toxicol 39 (1997) 214–219. [PubMed: 9251170]

[11]. Chaney LA, Wineman RW, Rockhold RW, Hume AS, Acute effects of an insect repellent, N, N-diethyl-m-toluamide, on cholinesterase inhibition induced by pyridostigmine bromide in rats, Toxicol. Appl. Pharmacol 165 (2000) 107–114, 10.1006/taap.2000.8936. [PubMed: 10828206]

[12]. Prendergast MA, Terry AV Jr., Buccafusco JJ, Chronic, low-level exposure to diisopropylfluorophosphate causes protracted impairment of spatial navigation learning, Psychopharmacology 129 (1997) 183–191, 10.1007/s002130050179. [PubMed: 9040125]

[13]. Terry AV Jr., Stone JD, Buccafusco JJ, Sickles DW, Sood A, Prendergast MA, Repeated exposures to subthreshold doses of chlorpyrifos in rats: hippocampal damage, impaired axonal transport, and deficits in spatial learning, J. Pharmacol. Exp. Ther 305 (2003) 375–384, 10.1124/jpet.102.041897. [PubMed: 12649392]

[14]. Abou-Donia MB, Wilmarth KR, Abdel-Rahman AA, Jensen KF, Oehme FW, Kurt TL, Increased neurotoxicity following concurrent exposure to pyridostigmine bromide, DEET, and chlorpyrifos, Fundam. Appl. Toxicol 34 (1996) 201–222, 10.1006/faat.1996.0190.

[15]. Ojo JO, Abdullah L, Evans J, Reed JM, Montague H, Mullan MJ, Crawford FC, Exposure to an organophosphate pesticide, individually or in combination with other gulf war agents, impairs synaptic integrity and neuronal differentiation, and is accompanied by subtle microvascular injury in a mouse model of gulf war agent exposure, Neuropathology 34 (2014) 109–127, 10.1111/neup.12061. [PubMed: 24118348]

[16]. Shetty GA, Hattiangady B, Upadhya D, Bates A, Attaluri S, Shuai B, Kodali M, Shetty AK, Chronic oxidative stress, mitochondrial dysfunction, Nrf2 activation and inflammation in the hippocampus accompany heightened systemic inflammation and oxidative stress in an animal model of gulf war illness, Front. Mol. Neurosci 10 (2017) 182, 10.3389/fnmol.2017.00182. [PubMed: 28659758]

[17]. Pierce LM, Kurata WE, Matsumoto KW, Clark ME, Farmer DM, Long-term epigenetic alterations in a rat model of gulf war illness, Neurotoxicology 55 (2016) 20–32, 10.1016/j.neuro.2016.05.007. [PubMed: 27179617]

[18]. Ashbrook DG, Hing B, Michalovicz LT, Kelly KA, Miller JV, de Vega WC, Miller DB, Broderick G, O'Callaghan JP, McGowan PO, Epigenetic impacts of stress priming of the neuroinflammatory response to sarin surrogate in mice: a model of gulf war illness, J. Neuroinflammation 15 (2018) 86, 10.1186/s12974-018-1113-9. [PubMed: 29549885]

[19]. Xu F, Ashbrook DG, Gao J, Starlard-Davenport A, Zhao W, Miller DB, O'Callaghan JP, Williams RW, Jones BC, Lu L, Genome-wide transcriptome architecture in a mouse model of gulf war illness, Brain Behav. Immun 89 (2020) 209–223, 10.1016/j.bbi.2020.06.018. [PubMed: 32574576]

[20]. Epstein I, Finkbeiner S, The arc of cognition: signaling cascades regulating arc and implications for cognitive function and disease, Semin. Cell Dev. Biol 77 (2018) 63–72, 10.1016/j.semcdb.2017.09.023. [PubMed: 29559111]

[21]. Korb E, Finkbeiner S, Arc in synaptic plasticity: from gene to behavior, Trends Neurosci 34 (2011) 591–598, 10.1016/j.tins.2011.08.007. [PubMed: 21963089]

[22]. Plath N, Ohana O, Dammermann B, Errington ML, Schmitz D, Gross C, Mao X, Engelsberg A, Mahlke C, Welzl H, Kobalz U, Stawrakakis A, Fernandez E, Waltereit R, Bick-Sander A, Therstappen E, Cooke SF, Blanquet V, Wurst W, Salmen B, Bosl MR, Lipp HP, Grant SG, Bliss TV, Wolfer DP, Kuhl D, Arc/Arg3.1 is essential for the consolidation of synaptic plasticity and memories, Neuron 52 (2006) 437–444, 10.1016/j.neuron.2006.08.024. [PubMed: 17088210]

[23]. Guzowski JF, Lyford GL, Stevenson GD, Houston FP, McGaugh JL, Worley PF, Barnes CA, Inhibition of activity-dependent arc protein expression in the rat hippocampus impairs the maintenance of long-term potentiation and the consolidation of long-term memory, J. Neurosci 20 (2000) 3993–4001. [PubMed: 10818134]

[24]. Jones MW, Errington ML, French PJ, Fine A, Bliss TV, Garel S, Charnay P, Bozon B, Laroche S, Davis S, A requirement for the immediate early gene Zif268 in the expression of late LTP and long-term memories, Nat. Neurosci 4 (2001) 289–296, 10.1038/85138. [PubMed: 11224546]

[25]. Li L, Carter J, Gao X, Whitehead J, Tourtellotte WG, The neuroplasticity-associated arc gene is a direct transcriptional target of early growth response (Egr) transcription factors, Mol. Cell. Biol 25 (2005) 10286–10300, 10.1128/MCB.25.23.10286-10300.2005. [PubMed: 16287845]

[26]. Perusini JN, Cajigas SA, Cohensedgh O, Lim SC, Pavlova IP, Donaldson ZR, Denny CA, Optogenetic stimulation of dentate gyrus engrams restores memory in Alzheimer's disease mice, Hippocampus 27 (2017) 1110–1122, 10.1002/hipo.22756. [PubMed: 28667669]

[27]. Dickey CA, Loring JF, Montgomery J, Gordon MN, Eastman PS, Morgan D, Selectively reduced expression of synaptic plasticity-related genes in amyloid precursor protein presenilin-1 transgenic mice, J. Neurosci 23 (2003) 5219–5226. [PubMed: 12832546]

[28]. Palop JJ, Chin J, Bien-Ly N, Massaro C, Yeung BZ, Yu GQ, Mucke L, Vulnerability of dentate granule cells to disruption of arc expression in human amyloid precursor protein transgenic mice, J. Neurosci 25 (2005) 9686–9693, 10.1523/JNEUROSCI.2829-05.2005. [PubMed: 16237173]

[29]. Rosi S, Ramirez-Amaya V, Vazdarjanova A, Worley PF, Barnes CA, Wenk GL, Neuroinflammation alters the hippocampal pattern of behaviorally induced arc expression, J. Neurosci 25 (2005) 723–731, 10.1523/JNEUROSCI.4469-04.2005. [PubMed: 15659610]

[30]. Perry KW, Nisenbaum LK, George CA, Shannon HE, Felder CC, Bymaster FP, The muscarinic agonist xanomeline increases monoamine release and immediate early gene expression in the rat prefrontal cortex, Biol. Psychiatry 49 (2001) 716–725, 10.1016/s0006-3223(00)01017-9. [PubMed: 11313039]

[31]. Tong XK, Lecrux C, Rosa-Neto P, Hamel E, Age-dependent rescue by simvastatin of Alzheimer's disease cerebrovascular and memory deficits, J. Neurosci 32 (2012) 4705–4715, 10.1523/JNEUROSCI.0169-12.2012. [PubMed: 22492027]

[32]. Gallitano AL, Editorial: the role of immediate early genes in neuropsychiatric illness, Front. Behav. Neurosci 14 (2020) 16, 10.3389/fnbeh.2020.00016. [PubMed: 32153372]

[33]. Duclot F, Kabbaj M, The role of early growth response 1 (EGR1) in brain plasticity and neuropsychiatric disorders, Front. Behav. Neurosci 11 (2017) 35, 10.3389/fnbeh.2017.00035. [PubMed: 28321184]

[34]. Xu Y, Pan J, Sun J, Ding L, Ruan L, Reed M, Yu X, Klabnik J, Lin D, Li J, Chen L, Zhang C, Zhang H, O'Donnell JM, Inhibition of phosphodiesterase 2 reverses impaired cognition and neuronal remodeling caused by chronic stress, Neurobiol. Aging 36 (2015) 955–970, 10.1016/j.neurobiolaging.2014.08.028. [PubMed: 25442113]

[35]. Covington HE 3rd, Lobo MK, Maze I, Vialou V, Hyman JM, Zaman S, LaPlant Q, Mouzon E, Ghose S, Tamminga CA, Neve RL, Deisseroth K, Nestler EJ, Antidepressant effect of optogenetic stimulation of the medial prefrontal cortex, J. Neurosci 30 (2010) 16082–16090, 10.1523/JNEUROSCI.1731-10.2010. [PubMed: 21123555]

[36]. Gallo FT, Katche C, Morici JF, Medina JH, Weisstaub NV, Immediate early genes, memory and psychiatric disorders: focus on c-fos, Egr1 and arc, Front. Behav. Neurosci 12 (2018) 79, 10.3389/fnbeh.2018.00079. [PubMed: 29755331]

[37]. Li Y, Pehrson AL, Waller JA, Dale E, Sanchez C, Gulinello M, A critical evaluation of the activity-regulated cytoskeleton-associated protein (Arc/Arg3.1)& apos;s putative role in regulating dendritic plasticity, cognitive processes, and mood in animal models of depression, Front. Neurosci 279 (2015), 10.3389/fnins.2015.00279.

[38]. Park AY, Park YS, So D, Song IK, Choi JE, Kim HJ, Lee KJ, Activity-regulated cytoskeleton-associated protein(Arc/Arg3.1) is transiently expressed after heat shock stress and suppresses heat shock factor 1, Sci. Rep 9 (2019) 2592, 10.1038/s41598-019-39292-1. [PubMed: 30796345]

[39]. Atkins CM, Yon M, Groome NP, Sweatt JD, Regulation of myelin basic protein phosphorylation by mitogen-activated protein kinase during increased action potential firing in the hippocampus, J. Neurochem 73 (1999) 1090–1097, 10.1046/j.1471-4159.1999.0731090.x. [PubMed: 10461899]

[40]. Lee PR, Fields RD, Regulation of myelin genes implicated in psychiatric disorders by functional activity in axons, Front. Neuroanat 3 (2009) 4, 10.3389/neuro.05.004.2009. [PubMed: 19521541]

[41]. Abou-Donia MB, Conboy LA, Kokkotou E, Jacobson E, Elmasry EM, Elkafrawy P, Neely M, Bass CR, Sullivan K, Screening for novel central nervous system biomarkers in veterans with gulf war illness, Neurotoxicol. Teratol 61 (2017) 36–46, 10.1016/j.ntt.2017.03.002. [PubMed: 28286177]

[42]. Abou-Donia MB, Lapadula ES, Krengel MH, Quinn E, LeClair J, Massaro J, Conboy LA, Kokkotou E, Abreu M, Klimas NG, Nguyen DD, Sullivan K, Using plasma autoantibodies of central nervous system proteins to distinguish veterans with gulf war illness from healthy and symptomatic controls, Brain Sci 10 (2020), 10.3390/brainsci10090610.

[43]. Carreras I, Aytan N, Mellott T, Choi JK, Lehar M, Crabtree L, Leite-Morris K, Jenkins BG, Blusztajn JK, Dedeoglu A, Anxiety, neuroinflammation, cholinergic and GABAergic abnormalities are early markers of gulf war illness in a mouse model of the disease, Brain Res 1681 (2018) 34–43, 10.1016/j.brainres.2017.12.030. [PubMed: 29277710]

[44]. Mauck B, Lucot JB, Paton S, Grubbs RD, Cholinesterase inhibitors and stress: effects on brain muscarinic receptor density in mice, Neurotoxicology 31 (2010) 461–467, 10.1016/j.neuro.2010.06.001. [PubMed: 20542057]

[45]. Abdullah L, Crynen G, Reed J, Bishop A, Phillips J, Ferguson S, Mouzon B, Mullan M, Mathura V, Mullan M, Ait-Ghezala G, Crawford F, Proteomic CNS profile of delayed cognitive impairment in mice exposed to gulf war agents, Neuromolecular Med 13 (2011) 275–288, 10.1007/s12017-011-8160-z. [PubMed: 21986894]

[46]. Abdel-Rahman A, Shetty AK, Abou-Donia MB, Disruption of the blood-brain barrier and neuronal cell death in cingulate cortex, dentate gyrus, thalamus, and hypothalamus in a rat model of gulf-war syndrome, Neurobiol. Dis 10 (2002) 306–326, 10.1006/nbdi.2002.0524. [PubMed: 12270692]

[47]. Friedman A, Kaufer D, Shemer J, Hendler I, Soreq H, Tur-Kaspa I, Pyridostigmine brain penetration under stress enhances neuronal excitability and induces early immediate transcriptional response, Nat. Med 2 (1996) 1382–1385, 10.1038/nm1296-1382. [PubMed: 8946841]

[48]. Keil DE, McGuinn WD, Dudley AC, EuDaly JG, Gilkeson GS, Peden-Adams MM, N, N,-diethyl-m-toluamide (DEET) suppresses humoral immunological function in B6C3F1 mice, Toxicol. Sci 108 (2009) 110–123, 10.1093/toxsci/kfp001. [PubMed: 19141786]

[49]. Lamproglou I, Barbier L, Diserbo M, Fauvelle F, Fauquette W, Amourette C, Repeated stress in combination with pyridostigmine part I: long-term behavioural consequences, Behav. Brain Res 197 (2009) 301–310, 10.1016/j.bbr.2008.08.031. [PubMed: 18793677]

[50]. Peden-Adam MM, Eudaly J, Eudaly E, Dudley A, Zeigler J, Lee A, Robbs J, Gilkeson G, Keil DE, Evaluation of immunotoxicity induced by single or concurrent exposure to N, N-diethyl-m-toluamide (DEET), pyridostigmine bromide (PYR), and JP-8 jet fuel, Toxicol. Ind. Health 17 (2001) 192–209, 10.1191/0748233701th120oa. [PubMed: 12539864]

[51]. Torres-Altoro MI, Mathur BN, Drerup JM, Thomas R, Lovinger DM, O'Callaghan JP, Bibb JA, Organophosphates dysregulate dopamine signaling, glutamatergic neurotransmission, and induce neuronal injury markers in striatum, J. Neurochem 119 (2011) 303–313, 10.1111/j.1471-4159.2011.07428.x. [PubMed: 21848865]

[52]. Craddock TJ, Harvey JM, Nathanson L, Barnes ZM, Klimas NG, Fletcher MA, Broderick G, Using gene expression signatures to identify novel treatment strategies in gulf war illness, BMC Med. Genet 8 (2015) 36, 10.1186/s12920-015-0111-3.

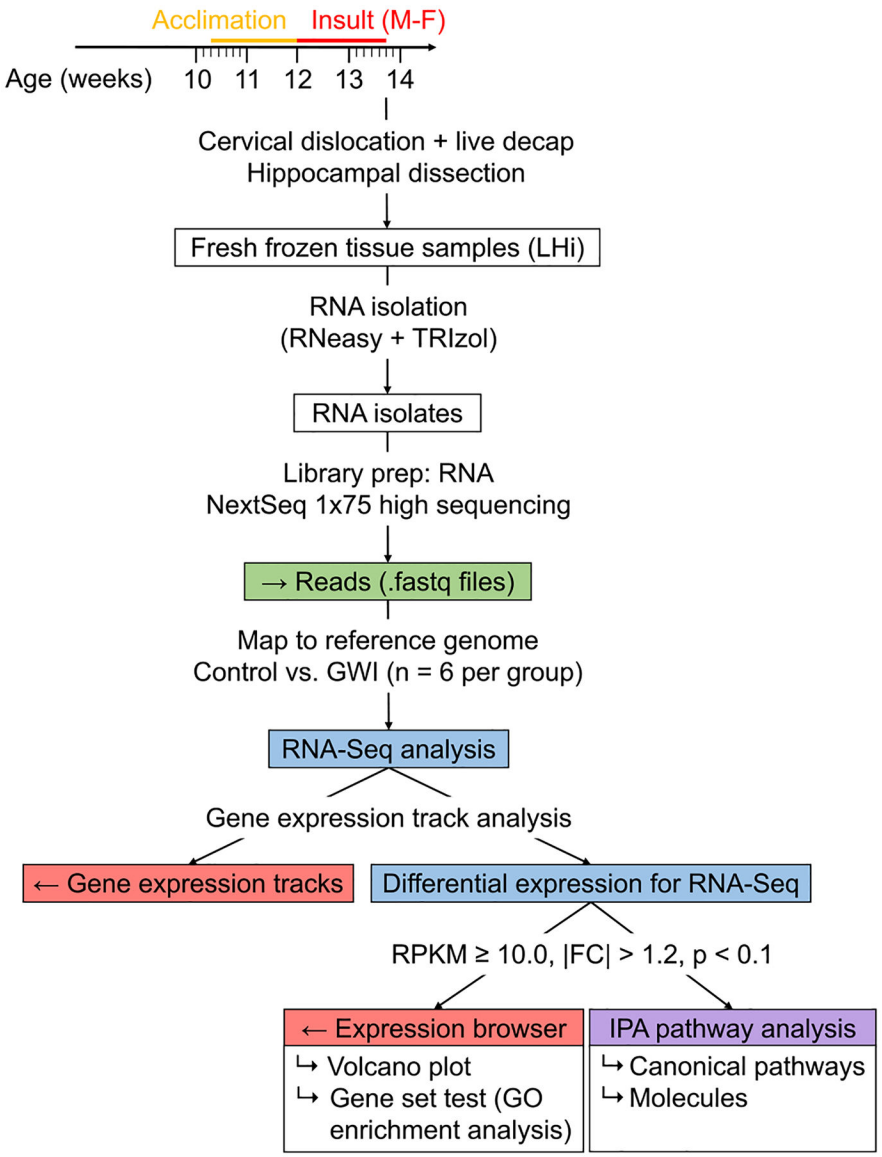

Fig. 1.

RNA-Seq analysis workflow with CLC Genomics Workbench and Ingenuity Pathway Analysis. Whole transcriptome sequencing was performed using mouse hippocampal RNA isolates collected 2–4 h after final exposure. Gene expression tracks were analyzed using the Differential Expression for RNA-Seq tool with RPKM >10.0, |FC| ≥ 1.2, and $p < 0.1$ as criteria for significance. GO enrichment analysis was performed on subset of genes that were significantly dysregulated. Data for significant genes was exported to Ingenuity Pathway Analysis to assess canonical pathways, molecules, diseases and functions, and other relevant information.

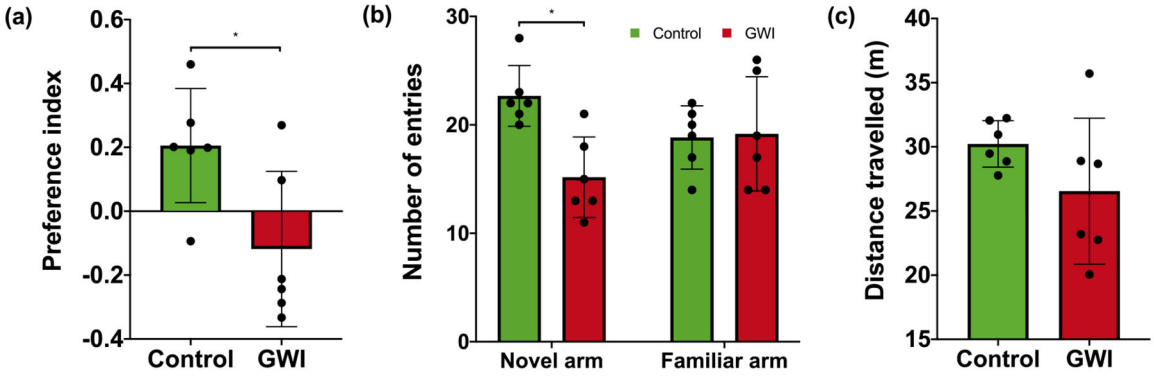

Fig. 2.

(a) Preference for novel arm, (b) number of entries per arm, and (c) distance travelled during trial phase of Y-maze. Hippocampal-dependent spatial memory was assessed by performance on a Y-maze task 2–4 h after final exposure. (a) Preference for the novel arm was significantly lower in mice receiving PB + CPF + DEET (mean = −0.12 ± 0.099) compared to control mice (mean = 0.21 ± 0.073) ($t(9.18) = 2.63$, $p = 0.027$). (b) The number of entries into the novel arm was also significantly lower in mice exposed to PB + CPF + DEET (mean = 15.2 ± 1.15) compared to controls (mean = 22.7 ± 1.52) ($t(9.31) = 3.95$, $p = 0.0031$). (c) Distance travelled during the test stage did not significantly differ between conditions (PB + CPF + DEET: mean = 26.6 ± 2.32, control: mean = 30.2 ± 0.74, $t(6.00) = 1.51$, $p = 0.18$). All results are graphed as mean ± SEM.

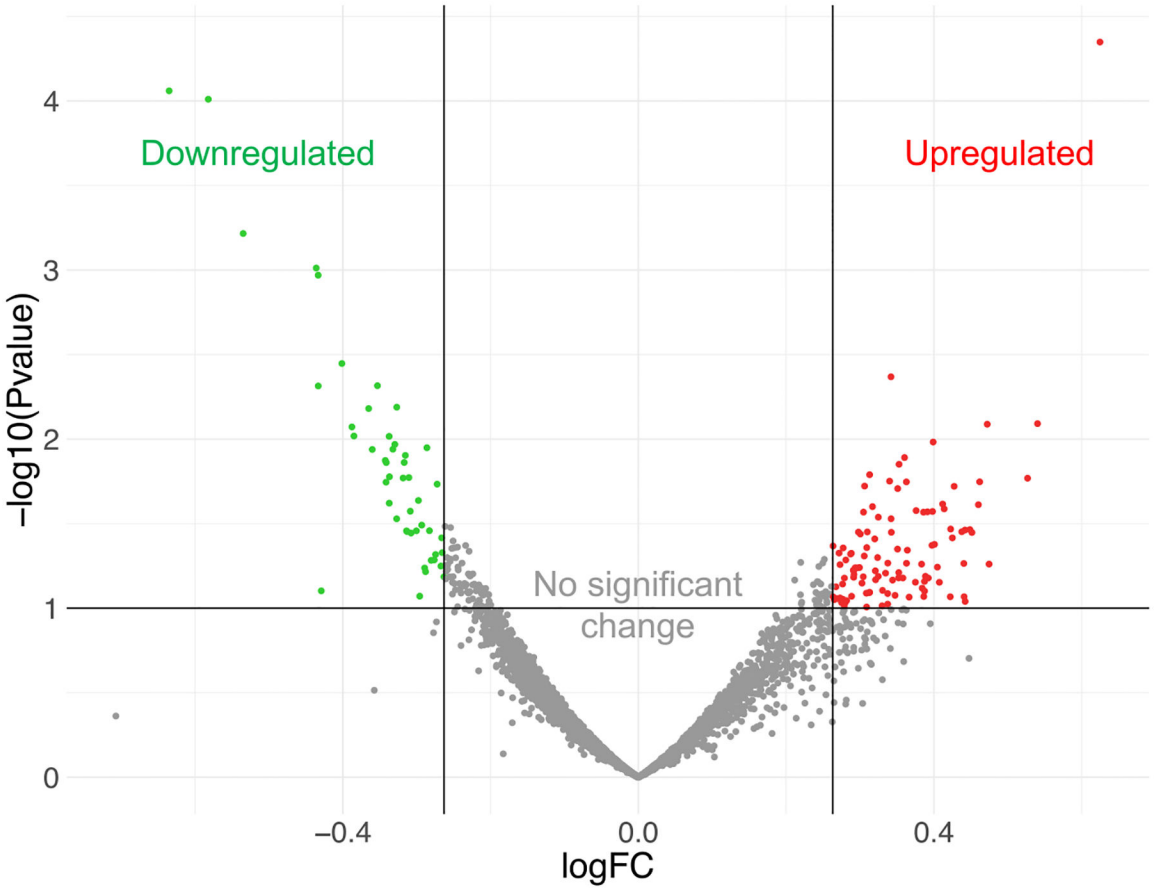

Fig. 3.

Differentially expressed genes identified by RNA-Seq analysis. Sequence counts from the RNA samples were evaluated with CLC Genomics Workbench and Ingenuity Pathway Analysis software. 158 dysregulated genes were identified in mice exposed to PB + CPF + DEET vs. controls. Genes were considered to be significantly dysregulated if they met the following criteria: RPKM >10.0, |fold change| ≥ 1.2, $p < 0.1$. Green = downregulated; red = upregulated.

Table 1

Downregulated genes after exposure to Gulf War insult. Green, negative fold changes indicate downregulation.

Symbol	Entrez Gene Name	RPKM	FC	P-value
Arc	Activity regulated cytoskeleton associated protein	33.6	−1.553	8.72E-05
Egr1	Early growth response 1	23.3	−1.497	9.77E-05
Nr4a1	Nuclear receptor subfamily 4 group A member 1	16.5	−1.449	0.000608
Apod	Apolipoprotein D	32.5	−1.353	0.000973
Hba-a2	Hemoglobin alpha, adult chain 2	60.7	−1.350	0.00485
Tmem88b	Transmembrane protein 88B	16.5	−1.350	0.00107
Wfs1	Wolframin ER transmembrane glycoprotein	33.2	−1.321	0.00357
Junb	JunB proto-oncogene, AP-1 transcription factor subunit	36.6	−1.308	0.00847
Fam163b	Family with sequence similarity 163 member B	52.3	−1.306	0.00959
Mog	Myelin oligodendrocyte glycoprotein	22.7	−1.288	0.00659
Mbp	Myelin basic protein	281.4	−1.284	0.0115
Bcas1	Breast carcinoma amplified sequence 1	41.5	−1.277	0.00483
Cd9	CD9 molecule	29.2	−1.268	0.0134
Gsn	Gelsolin	15.9	−1.267	0.0138
Pllp	Plasmolipin	21.3	−1.267	0.018
Mag	Myelin associated glycoprotein	50.6	−1.263	0.00963
Nutf2-ps1	Nuclear transport factor 2, pseudogene 1	19.1	−1.263	0.0167
Pcp4l1	Purkinje cell protein 4-like 1	26.7	−1.263	0.0239
H2-D1	Histocompatibility 2, D region locus 1	11.8	−1.259	0.0115
Trf	Transferrin	62.8	−1.257	0.0107
Rpl10-ps3	Ribosomal protein L10, pseudogene 3	75.6	−1.255	0.0296
Plekhb1	Pleckstrin homology domain containing B1	65.3	−1.254	0.00647
Srebf1	Sterol regulatory element binding transcription factor 1	11.2	−1.247	0.017
Cnp	2’,3’-cyclic nucleotide 3’ phosphodiesterase	105.7	−1.246	0.0137
Septin4	Septin 4	27.6	−1.244	0.0125
Slco1c1	Solute carrier organic anion transporter family member 1C1	11.2	−1.243	0.0349
Pltp	Phospholipid transfer protein	21.6	−1.242	0.0352
Cldn11	Claudin 11	73.5	−1.240	0.0169

Symbol	Entrez Gene Name	RPKM	FC	P-value
Fa2h	Fatty acid 2-hydroxylase	11.0	−1.239	0.0267
Rhog	Ras homolog family member G	12.3	−1.238	0.0359
Prr18	Proline rich 18	17.0	−1.229	0.0231
Egr4	Early growth response 4	16.8	−1.228	0.0849
mt-Atp8	ATP synthase F0 subunit 8	7509.7	−1.225	0.0323
C1ql2	Complement C1q like 2	40.4	−1.222	0.0578
Nfkbia	NFKB inhibitor alpha	12.4	−1.221	0.0608
Igfbp5	Insulin like growth factor binding protein 5	23.2	−1.219	0.0112
B2m	Beta-2-microglobulin	57.4	−1.217	0.0348
Hbb-bs	Hemoglobin subunit beta	45.2	−1.215	0.0521
S100a16	S100 calcium binding protein A16	20.3	−1.211	0.0518
mt-Atp6	ATP synthase F0 subunit 6	8936.0	−1.210	0.0481
Slc6a6	Solute carrier family 6 member 6	15.6	−1.208	0.0185
Ddit4	DNA damage inducible transcript 4	38.8	−1.204	0.0563
Anxa5	Annexin A5	15.5	−1.203	0.0383
S100a1	S100 calcium binding protein A1	35.3	−1.202	0.0469
Chrm3	Cholinergic receptor muscarinic 3	10.5	−1.200	0.0652

Table 2

Upregulated genes after exposure to Gulf War insult. Red, positive fold changes indicate upregulation.

Symbol	Entrez Gene Name	RPKM	FC	P-value
Lars2	Leucyl-tRNA synthetase 2, mitochondrial	744.328	1.542	4.48E-05
Gdf1	Growth differentiation factor 1	11.348	1.454	0.0081
Cdr1	Cerebellar degeneration related antigen 1	23.178	1.441	0.017
Fam126b	Family with sequence similarity 126 member B	12.032	1.390	0.0548
Pak3	p21 (RAC1) activated kinase 3	14.277	1.387	0.00816
Igip	IgA inducing protein	31.362	1.377	0.0179
Pgm2l1	Phosphoglucomutase 2 like 1	45.308	1.376	0.0244
Smc3	Structural maintenance of chromosomes 3	11.216	1.367	0.0357
Dgkb	Diacylglycerol kinase beta	20.952	1.365	0.0343
Atrx	ATRX chromatin remodeler	10.147	1.359	0.0912
Ppp4r2	Protein phosphatase 4 regulatory subunit 2	14.623	1.359	0.0345
Ankrd12	Ankyrin repeat domain 12	10.712	1.357	0.0856
Hspa4l	Heat shock protein family A (Hsp70) member 4 like	12.354	1.357	0.0544
Ppig	Peptidylprolyl isomerase G	11.563	1.354	0.0353
Rabep1	Rabaptin, RAB GTPase binding effector protein 1	16.266	1.345	0.019
Dnajb4	DnaJ heat shock protein family (Hsp40) member B4	11.871	1.343	0.0384
Pcmtd1	Protein-L-isoaspartate (D-aspartate) O-methyltransferase domain containing 1	16.76	1.340	0.0856
Reps2	RALBP1 associated Eps domain containing 2	21.405	1.340	0.034
Ube2q2	Ubiquitin conjugating enzyme E2 Q2	13.79	1.332	0.0259
Rab3c	RAB3C, member RAS oncogene family	44.551	1.330	0.0242
Acbd5	Acyl-CoA binding domain containing 5	11.406	1.326	0.0703
Fmr1	FMRP translational regulator 1	11.502	1.324	0.0571
Tax1bp1	Tax1 binding protein 1	22.074	1.320	0.0419
Nus1	NUS1 dehydrodolichyl diphosphate synthase subunit	16.346	1.319	0.0104
Hsp90aa1	Heat shock protein 90 alpha family class A member 1	213.841	1.318	0.0268
Gmfb	Glia maturation factor beta	35.439	1.317	0.0425
Gpbp1	GC-rich promoter binding protein 1	17.787	1.313	0.0663
Naa50	N(alpha)-acetyltransferase 50, NatE catalytic subunit	16.618	1.312	0.0269

Symbol	Entrez Gene Name	RPKM	FC	P-value
Gabra2	Gamma-aminobutyric acid type A receptor alpha2 subunit	36.465	1.309	0.0647
Fxr1	FMR1 autosomal homolog 1	11.598	1.308	0.0792
Kpna3	Karyopherin subunit alpha 3	16.133	1.308	0.0695
Ipo7	Importin 7	17.7	1.307	0.0853
Mphosph8	M-phase phosphoprotein 8	15.901	1.307	0.027
Kif5b	Kinesin family member 5B	33.739	1.305	0.0762
Psd3	Pleckstrin and Sec7 domain containing 3	26.285	1.304	0.0549
Pde1a	Phosphodiesterase 1A	26.28	1.298	0.0265
Mob4	MOB family member 4, phocein	14.856	1.297	0.0703
Uba3	Ubiquitin like modifier activating enzyme 3	13.952	1.289	0.086
Slc8a1	Solute carrier family 8 member A1	11.848	1.287	0.0454
Ankrd13c	Ankyrin repeat domain 13C	19.116	1.286	0.0179
Pten	Phosphatase and tensin homolog	20.14	1.286	0.0542
Eif3a	Eukaryotic translation initiation factor 3 subunit A	27.913	1.284	0.0128
Gabrb1	Gamma-aminobutyric acid type A receptor beta1 subunit	13.845	1.282	0.0663
Ogfrl1	Opioid growth factor receptor like 1	36.947	1.277	0.0141
Selenot	Selenoprotein T	44.851	1.277	0.0616
Eif5	Eukaryotic translation initiation factor 5	34.859	1.276	0.0662
Htatsf1	HIV-1 Tat specific factor 1	18.843	1.275	0.0447
Top1	DNA topoisomerase I	22.617	1.275	0.0196
Slc25a46	Solute carrier family 25 member 46	11.765	1.272	0.084
Nrxn1	Neurexin 1	30.941	1.269	0.0682
Gad2	Glutamate decarboxylase 2	17.309	1.268	0.0356
Fgfr1op2	FGFR1 oncogene partner 2	25.756	1.267	0.0296
Hspa5	Heat shock protein family A (Hsp70) member 5	46.918	1.267	0.00428
Zc3h15	Zinc finger CCCH-type containing 15	34.721	1.266	0.0177
Armcx3	Armadillo repeat containing X-linked 3	22	1.264	0.0541
Hnrnpa3	Heterogeneous nuclear ribonucleoprotein A3	29.364	1.263	0.0946
Senp6	SUMO specific peptidase 6	10.207	1.263	0.0819
Fbxo11	F-box protein 11	23.116	1.261	0.062
Cert1	Ceramide transporter 1	11.829	1.257	0.0968

Symbol	Entrez Gene Name	RPKM	FC	P-value
Oxr1	Oxidation resistance 1	23.222	1.257	0.0785
Impact	Impact RWD domain protein	38.33	1.252	0.0648
Psip1	PC4 and SFRS1 interacting protein 1	32.895	1.252	0.0289
Slmap	Sarcolemma associated protein	13.2	1.252	0.0502
Fgf12	Fibroblast growth factor 12	10.635	1.249	0.0679
Sucla2	Succinate-CoA ligase ADP-forming beta subunit	33.008	1.249	0.0601
Dld	Dihydrolipoamide dehydrogenase	28.74	1.248	0.0389
Negr1	Neuronal growth regulator 1	18.551	1.246	0.0251
Acsl4	Acyl-CoA synthetase long chain family member 4	13.462	1.242	0.0806
Dnaja1	DnaJ heat shock protein family (Hsp40) member A1	37.903	1.242	0.0162
Pnrc2	Proline rich nuclear receptor coactivator 2	13.435	1.242	0.0808
Eif5b	Eukaryotic translation initiation factor 5B	11.453	1.240	0.0354
Mib1	Mindbomb E3 ubiquitin protein ligase 1	15.309	1.239	0.0985
Plcb1	Phospholipase C beta 1	19.494	1.239	0.0438
Map9	Microtubule associated protein 9	15.383	1.238	0.0815
Jakmip2	Janus kinase and microtubule interacting protein 2	11.357	1.236	0.0491
Pura	Purine rich element binding protein A	19.084	1.236	0.019
Hsp90b1	Heat shock protein 90 beta family member 1	65.468	1.235	0.027
Ncl	Nucleolin	18.087	1.235	0.0652
Neto1	Neuropilin and tolloid like 1	16.105	1.233	0.0711
Gda	Guanine deaminase	30.573	1.232	0.0364
Cnr1	Cannabinoid receptor 1	25.574	1.231	0.0575
Bhlhb9	Basic helix-loop-helix family member b9	16.07	1.229	0.0355
Ythdc1	YTH domain containing 1	13.542	1.228	0.0578
Golga4	Golgin A4	10.017	1.226	0.0576
Cir1	Corepressor interacting with RBPJ, 1	10.903	1.224	0.0657
Mzt1	Mitotic spindle organizing protein 1	27.367	1.224	0.0631
Rnf6	Ring finger protein 6	10.488	1.224	0.0599
Gdap1	Ganglioside induced differentiation associated protein 1	20.359	1.223	0.0596
Lpgat1	Lysophosphatidylglycerol acyltransferase 1	20.943	1.221	0.0473
Pin4	Peptidylprolyl cis/trans isomerase, NIMA-interacting 4	14.967	1.221	0.085

Symbol	Entrez Gene Name	RPKM	FC	P-value
Cpne7	Copine 7	93.847	1.220	0.0478
Ggnbp2	Gametogenetin binding protein 2	18.355	1.216	0.0902
Etv1	ETS variant transcription factor 1	14.066	1.215	0.0518
Arl5a	ADP ribosylation factor like GTPase 5A	15.424	1.214	0.0924
Pafah1b1	Platelet activating factor acetylhydrolase 1b regulatory subunit 1	59.969	1.213	0.0964
Tafa1	TAFA chemokine like family member 1	11.298	1.213	0.0663
Srsf3	Serine and arginine rich splicing factor 3	27.672	1.212	0.044
Tceal9	Transcription elongation factor A like 9	29.46	1.212	0.0939
Ccdc47	Coiled-coil domain containing 47	14.385	1.211	0.0885
Tim2	Tripartite motif containing 2	46.277	1.211	0.072
Aff4	AF4/FMR2 family member 4	15.746	1.210	0.093
C5orf24	Chromosome 5 open reading frame 24	18.903	1.210	0.0917
Msantd4	Myb/SANT DNA binding domain containing 4 with coiled-coils	14.084	1.208	0.0552
Rab39b	RAB39B, member RAS oncogene family	10.444	1.208	0.087
Vxn	Vexin	56.093	1.207	0.0472
Tmem33	Transmembrane protein 33	10.859	1.205	0.0876
Slk	STE20 like kinase	10.826	1.204	0.0747
Hdgfl3	HDGF like 3	11.325	1.202	0.0891
Dynlt3	Dynein light chain Tctex-type 3	39.421	1.201	0.0859
Dyrk2	Dual specificity tyrosine phosphorylation regulated kinase 2	10.698	1.200	0.0429

Table 3

Significantly affected canonical pathways after Gulf War insult. Green, negative fold changes indicate downregulation. Red, positive fold changes indicate upregulation.

Ingenuity Canonical Pathways	−log(p-value)	Ratio	Molecules
Protein Ubiquitination Pathway	4.08	0.033	B2m, Dnaja1, Dnajb4, Hba-a2, Hsp90aa1, Hsp90b1, Hspa4l, Hspa5, Ube2q2
Aldosterone Signaling in Epithelial Cells	4.07	0.0443	Dnaja1, Dnajb4, Hsp90aa1, Hsp90b1, Hspa4l, Hspa5, Plcb1
Hypoxia Signaling in the Cardiovascular System	3.9	0.0676	Hsp90aa1, Hsp90b1, Nfkbia, Pten, Ube2q2
Mitotic Roles of Polo-Like Kinase	3.03	0.0606	Hsp90aa1, Hsp90b1, Slk, Smc3
Prostate Cancer Signaling	2.51	0.044	Hsp90aa1, Hsp90b1, Nfkbia, Pten
Unfolded protein response	2.23	0.0536	Hsp90b1, Hspa5, Srebf1
Role of PKR in Interferon Induction and Antiviral Response	2.13	0.0342	Hsp90aa1, Hsp90b1, Hspa5, Nfkbia
Endoplasmic Reticulum Stress Pathway	2.08	0.0952	Hsp90b1, Hspa5
LXR/RXR Activation	2.08	0.0331	Apod, Pltp, Srebf1, Trf
FXR/RXR Activation	2.02	0.0317	Apod, Pltp, Srebf1, Trf
TCA Cycle II (Eukaryotic)	1.97	0.0833	Dld, Sucla2
Glutamate Dependent Acid Resistance	1.88	0.5	Gad2
EIF2 Signaling	1.79	0.0223	Eif3a, Eif5, Eif5b, Hspa5, Srebf1
Gαq Signaling	1.69	0.0253	Chrm3, Nfkbia, Plcb1, Rhog
Cytotoxic T Lymphocyte-mediated Apoptosis of Target Cells	1.68	0.0588	B2m, Hba-a2
eNOS Signaling	1.68	0.0252	Chrm3, Hsp90aa1, Hsp90b1, Hspa5
0X40 Signaling Pathway	1.67	0.0333	B2m, Hba-a2, Nfkbia
Regulation of Actin-based Motility by Rho	1.62	0.0319	Gsn, Pak3, Rhog
CXCR4 Signaling	1.61	0.024	Egr1, Pak3, Plcb1, Rhog
GABA Receptor Signaling	1.61	0.0316	Gabra2, Gabrb1, Gad2
Neuregulin Signaling	1.6	0.0312	Hsp90aa1, Hsp90b1, Pten
Branched-chain α-keto acid Dehydrogenase Complex	1.59	0.25	Dld
Antigen Presentation Pathway	1.57	0.0513	B2m, Hba-a2
Nitric Oxide Signaling in the Cardiovascular System	1.56	0.0303	Hsp90aa1, Hsp90b1, Pde1A
PI3K/AKT Signaling	1.55	0.0229	Hsp90aa1, Hsp90b1, Nfkbia, Pten
Sumoylation Pathway	1.52	0.0291	Nfkbia, Rhog, Senp6
PPAR Signaling	1.51	0.0288	Hsp90aa1, Hsp90b1, Nfkbia

Ingenuity Canonical Pathways	−log(p-value)	Ratio	Molecules
2-ketoglutarate Dehydrogenase Complex	1.49	0.2	Dld
2-oxobutanoate Degradation I	1.49	0.2	Dld
Glutamate Degradation III (via 4-aminobutyrate)	1.49	0.2	Gad2
BAG2 Signaling Pathway	1.49	0.0465	Hsp90aa1, Hspa5
Dendritic Cell Maturation	1.49	0.0219	B2m, Hba-a2, Nfkbia, Plcb1
PD-1, PD-L1 cancer immunotherapy pathway	1.49	0.0283	B2m, Hba-a2, Pten
G-Protein Coupled Receptor Signaling	1.47	0.0184	Chrm3, Cnr1, Nfkbia, Pde1A, Plcb1
Antioxidant Action of Vitamin C	1.45	0.0275	Nfkbia, Plcb1, Selenot
PPARα/RXRα Activation	1.44	0.0211	Hsp90aa1, Hsp90b1, Nfkbia, Plcb1
iCOS-iCOSL Signaling in T Helper Cells	1.44	0.027	Hba-a2, Nfkbia, Pten
Type I Diabetes Mellitus Signaling	1.44	0.027	Gad2, Hba-a2, Nfkbia
Glycine Cleavage Complex	1.41	0.167	Dld
Natural Killer Cell Signaling	1.39	0.0203	B2m, Hba-a2, Hspa5, Pak3
Role of Tissue Factor in Cancer	1.38	0.0256	Egr1, Plcb1, Pten
TNFR1 Signaling	1.37	0.04	Nfkbia, Pak3
Thioredoxin Pathway	1.35	0.143	Selenot
Acetyl-CoA Biosynthesis I (Pyruvate Dehydrogenase Complex)	1.35	0.143	Dld
Neuroinflammation Signaling Pathway	1.32	0.0167	B2m, Gabra2, Gabrb1, Gad2, Hba-a2

Table 4a

Subset of significantly affected gene ontology categories involved in biological processes. Green, negative fold changes indicate downregulation. Red, positive fold changes indicate upregulation.

GO term	Description	Detected Genes	DE Genes	DE Genes (Names)	P-values
0110077	Vesicle-mediated intercellular transport	1	1	Arc	2.89E-4
0006429	Leucyl-tRNA aminoacylation	2	1	Lars2	5.78E-4
0050767	Regulation of neurogenesis	934	3	Arc, Gh, Opalin	1.45E-3
0006518	Peptide metabolic process	262	2	Hmgn5, Lars2	2.22E-3
0090031	Positive regulation of steroid hormone biosynthetic process	9	1	Gh	2.60E-3
2000969	Positive regulation of alpha-amino-3-hydroxy-5-methyl-4-isoxazole propionate selective glutamate receptor activity	9	1	Arc	2.60E-3
0032094	Response to food	12	1	Gh	3.47E-3
0043603	Cellular amide metabolic process	392	2	Hmgn5, Lars2	4.90E-3
1900452	Regulation of long-term synaptic depression	17	1	Arc	4.91E-3
0007405	Neuroblast proliferation	19	1	Gh	5.48E-3
0099149	Regulation of postsynaptic neurotransmitter receptor internalization	23	1	Arc	6.64E-3
0032543	Mitochondrial translation	31	1	Lars2	8.94E-3
0007616	Long-term memory	39	1	Arc	0.0112
0007492	Endoderm development	40	1	Arc	0.0115
0040018	Positive regulation of multicellular organism growth	42	1	Gh	0.0121
0072089	Stem cell proliferation	45	1	Gh	0.0129
0048286	Lung alveolus development	49	1	Gh	0.0141
0048713	Regulation of oligodendrocyte differentiation	49	1	Opalin	0.0141
0010828	Positive regulation of glucose transport	50	1	Gh	0.0144
0051028	mRNA transport	52	1	Arc	0.0149
1900271	Regulation of long-term synaptic potentiation	54	1	Arc	0.0155
0006749	Glutathione metabolic process	55	1	Hmgn5	0.0158
0061001	Regulation of dendritic spine morphogenesis	56	1	Arc	0.0161
0099601	Regulation of neurotransmitter receptor activity	60	1	Arc	0.0172
0061351	Neural precursor cell proliferation	63	1	Gh	0.0181
0048168	Regulation of neuronal synaptic plasticity	69	1	Arc	0.0198
0045685	Regulation of glial cell differentiation	86	1	Opalin	0.0246

GO term	Description	Detected Genes	DE Genes	DE Genes (Names)	P-values
0032869	Cellular response to insulin stimulus	87	1	Gh	0.0249
0046889	Positive regulation of lipid biosynthetic process	94	1	Gh	0.0269
0060998	Regulation of dendritic spine development	97	1	Arc	0.0277
0032414	Positive regulation of ion transmembrane transporter activity	114	1	Arc	0.0325
0051260	Protein homooligomerization	116	1	Arc	0.0331
0071375	Cellular response to peptide hormone stimulus	119	1	Gh	0.0340
0006575	Cellular modified amino acid metabolic process	138	1	Hmgn5	0.0393
0014013	Regulation of gliogenesis	148	1	Opalin	0.0421
1901564	Organonitrogen compound metabolic process	1208	2	Hmgn5, Lars2	0.0423
0010469	Regulation of receptor activity	156	1	Arc	0.0443
0009952	Anterior/posterior pattern specification	170	1	Arc	0.0482
0043604	Amide biosynthetic process	214	1	Lars2	0.0604
0043933	Macromolecular complex subunit organization	1504	2	Arc, Hmgn5	0.0633
1901215	Negative regulation of neuron death	244	1	Gh	0.0686
0032412	Regulation of ion transmembrane transporter activity	249	1	Arc	0.0700
0006790	Sulfur compound metabolic process	271	1	Hmgn5	0.0760
0009416	Response to light stimulus	288	1	Gh	0.0806
0050890	Cognition	325	1	Arc	0.0905
0010769	Regulation of cell morphogenesis involved in differentiation	344	1	Arc	0.0956
0007005	Mitochondrion organization	345	1	Lars2	0.0959
0071417	9 Cellular response to organonitrogen compound	347	1	Gh	0.0964

Life Sci. Author manuscript; available in PMC 2022 April 09.

Table 4b

Subset of significantly affected gene ontology categories involved in molecular functions. Green, negative fold changes indicate downregulation. Red, positive fold changes indicate upregulation.

GO term	Description	Detected Genes	DE Genes	DE Genes (Names)	P-values
0033592	RNA strand annealing activity	3	2	Fmr1, Fxr1	2.18E-04
0097100	Supercoiled DNA binding	3	2	Psip1, Top1	2.18E-04
0070840	Dynein complex binding	21	3	Fmr1, Pafah1b1, Smc3	7.32E-04
0051082	Unfolded protein binding	61	4	Dnajb4, Hsp90aa1, Hsp90b1, Hspa5	1.85E-03
0002151	G-quadruplex RNA binding	9	2	Fmr1, Fxr1	2.52E-03
0062061	TAP complex binding	9	2	H2-D1, H2-K1	2.52E-03
0031720	Haptoglobin binding	9	2	Hba-a2, Hbb-bs	2.52E-03
0019911	Structural constituent of myelin sheath	10	2	Mbp, Pllp	3.14E-03
0030881	Beta-2-microglobulin binding	11	2	H2-D1, H2-K1	3.81E-03
0042610	CD8 receptor binding	11	2	H2-D1, H2-K1	3.81E-03
0046977	TAP binding	11	2	H2-D1, H2-K1	3.81E-03
0003743	Translation initiation factor activity	38	3	Eif3a, Eif5, Eif5b	4.18E-03
1990825	Sequence-specific mRNA binding	13	2	Fmr1, Srsf3	5.35E-03
0022851	GABA-gated chloride ion channel activity	13	2	Gabra2, Gabrb1	5.35E-03
0097001	Ceramide binding	14	2	Mag, Pltp	6.20E-03
0042608	T cell receptor binding	15	2	H2-D1, H2-K1	7.12E-03
0004113	2’,3’-cyclic-nucleotide 3’-phosphodiesterase activity	1	1	Cnp	8.57E-03
0004148	Dihydrolipoyl dehydrogenase activity	1	1	Dld	8.57E-03
0043544	Lipoamide binding	1	1	Dld	8.57E-03
0080132	Fatty acid alpha-hydroxylase activity	1	1	Fa2h	8.57E-03
0008892	Guanine deaminase activity	1	1	Gda	8.57E-03
0052858	Peptidyl-lysine acetyltransferase activity	1	1	Naa50	8.57E-03
1990631	ErbB-4 class receptor binding	1	1	Ncl	8.57E-03
0047933	Glucose-1,6-bisphosphate synthase activity	1	1	Pgm2l1	8.57E-03
0140339	Phosphatidylglycerol transfer activity	1	1	Pltp	8.57E-03
0140340	Cerebroside transfer activity	1	1	Pltp	8.57E-03
0140337	Diacylglyceride transfer activity	1	1	Pltp	8.57E-03

GO term	Description	Detected Genes	DE Genes	DE Genes (Names)	P-values
0140338	Sphingomyelin transfer activity	1	1	Pltp	8.57E-03
0051717	Inositol-1,3,4,5-tetrakisphosphate 3-phosphatase activity	1	1	Pten	8.57E-03
0051800	Phosphatidylinositol-3,4-bisphosphate 3-phosphatase activity	1	1	Pten	8.57E-03
0001761	Beta-alanine transmembrane transporter activity	1	1	Slc6a6	8.57E-03
0005369	Taurine:sodium symporter activity	1	1	Slc6a6	8.57E-03
0004890	GABA-A receptor activity	18	2	Gabra2, Gabrb1	0.010198
0019825	Oxygen binding	18	2	Hba-a2, Hbb-bs	0.010198
0031489	Myosin V binding	20	2	Rab39b, Rab3c	0.012524
0043022	Ribosome binding	57	3	Fmr1, Hspa5, Impact	0.01287
0008139	Nuclear localization sequence binding	21	2	Kpna3, Nfkbia	0.013765
0005104	Fibroblast growth factor receptor binding	22	2	Fgf12, Nrxn1	0.015057
0001671	ATPase activator activity	23	2	Dnaja1, Dnajb4	0.0164
0004351	Glutamate decarboxylase activity	2	1	Gad2	0.017065
0031722	Hemoglobin beta binding	2	1	Hbb-bs	0.017065
0002135	CTP binding	2	1	Hsp90aa1	0.017065
0099609	Microtubule lateral binding	2	1	Kif5b	0.017065
0004823	Leucine-tRNA ligase activity	2	1	Lars2	0.017065
0045547	Dehydrodolichyl diphosphate synthase activity	2	1	Nus1	0.017065
0120019	Phosphatidylcholine transfer activity	2	1	Pltp	0.017065
0030977	Taurine binding	2	1	Slc6a6	0.017065
0086038	Calcium:sodium antiporter activity involved in regulation of cardiac muscle cell membrane potential	2	1	Slc8a1	0.017065
0099580	Ion antiporter activity involved in regulation of postsynaptic membrane potential	2	1	Slc8a1	0.017065
0032810	Sterol response element binding	2	1	Srebf1	0.017065
0004775	Succinate-CoA ligase (ADP-forming) activity	2	1	Sucla2	0.017065
0034986	Iron chaperone activity	2	1	Trf	0.017065
0019781	NEDD8 activating enzyme activity	2	1	Uba3	0.017065
0048027	mRNA 5’-UTR binding	24	2	Fmr1, Ncl	0.017791
0044183	Protein folding chaperone	26	2	Hsp90aa1, Hspa5	0.020718
0035064	Methylated histone binding	70	3	Atrx, Fmr1, Mphosph8	0.022223
0048306	Calcium-dependent protein binding	70	3	Nrxn1, S100a1, Wfs1	0.022223
0042605	Peptide antigen binding	27	2	H2-D1, H2-K1	0.022251

GO term	Description	Detected Genes	DE Genes	DE Genes (Names)	P-values
0042165	Neurotransmitter binding	28	2	Chrm3, Slc6a6	0.02383
0050750	Low-density lipoprotein particle receptor binding	28	2	Dnaja1, Hsp90b1	0.02383
0008081	Phosphoric diester hydrolase activity	72	3	Cnp, Pde1a, Plcb1	0.023917
0004949	Cannabinoid receptor activity	3	1	Cnr1	0.025489
0044729	Hemi-methylated DNA-binding	3	1	Egr1	0.025489
0051033	RNA transmembrane transporter activity	3	1	Hnrnpa3	0.025489
0017098	Sulfonylurea receptor binding	3	1	Hsp90aa1	0.025489
1905576	Ganglioside GT1b binding	3	1	Mag	0.025489
0042134	rRNA primary transcript binding	3	1	Ncl	0.025489
0004719	Protein-L-isoaspartate (D-aspartate) O-methyltransferase activity	3	1	Pcmtd1	0.025489
0048101	Calcium-and calmodulin-regulated 3’,5’-cyclic-GMP phosphodiesterase activity	3	1	Pde1a	0.025489
0004117	Calmodulin-dependent cyclic-nucleotide phosphodiesterase activity	3	1	Pde1a	0.025489
0003681	Bent DNA binding	3	1	Pin4	0.025489
0016314	Phosphatidylinositol-3,4,5-trisphosphate 3-phosphatase activity	3	1	Pten	0.025489
0070139	SUMO-specific endopeptidase activity	3	1	Senp6	0.025489
1905060	Calcium:cation antiporter activity involved in regulation of postsynaptic cytosolic calcium ion concentration	3	1	Slc8a1	0.025489
0003917	DNA topoisomerase type I activity	3	1	Top1	0.025489
0071074	Eukaryotic initiation factor eIF2 binding	4	1	Eif5	0.033841
0031721	Hemoglobin alpha binding	4	1	Hbb-bs	0.033841
0032564	dATP binding	4	1	Hsp90aa1	0.033841
0032551	Pyrimidine ribonucleoside binding	4	1	Hsp90aa1	0.033841
0002134	UTP binding	4	1	Hsp90aa1	0.033841
0044547	DNA topoisomerase binding	4	1	Ncl	0.033841
0097109	Neuroligin family protein binding	4	1	Nrxn1	0.033841
0032422	Purine-rich negative regulatory element binding	4	1	Pura	0.033841
0015349	Thyroid hormone transmembrane transporter activity	4	1	Slco1c1	0.033841
0042162	Telomeric DNA binding	34	2	Ncl, Pura	0.03421
0031369	Translation initiation factor binding	35	2	Eif5, Fmr1	0.036084
0060590	ATPase regulator activity	37	2	Dnaja1, Dnajb4	0.039946
0070087	Chromo shadow domain binding	5	1	Atrx	0.042122
0015616	DNA translocase activity	5	1	Atrx	0.042122

GO term	Description	Detected Genes	DE Genes	DE Genes (Names)	P-values
0055131	C3HC4-type RING finger domain binding	5	1	Dnaja1	0.042122
0005131	Growth hormone receptor binding	5	1	Gh	0.042122
0051022	Rho GDP-dissociation inhibitor binding	5	1	Hsp90aa1	0.042122
0005105	Type 1 fibroblast growth factor receptor binding	5	1	Nrxn1	0.042122
0036033	Mediator complex binding	5	1	Smc3	0.042122
0035255	Ionotropic glutamate receptor binding	39	2	Neto1, Pten	0.043957
0047676	Arachidonate-CoA ligase activity	6	1	Acsl4	0.050333
0016907	G-protein coupled acetylcholine receptor activity	6	1	Chrm3	0.050333
0034604	Pyruvate dehydrogenase (NAD+) activity	6	1	Dld	0.050333
0035368	Selenocysteine insertion sequence binding	6	1	Ncl	0.050333
0019992	Diacylglycerol binding	6	1	Pltp	0.050333
1990050	Phosphatidic acid transporter activity	6	1	Pltp	0.050333
1904121	Phosphatidylethanolamine transporter activity	6	1	Pltp	0.050333
0004791	Thioredoxin-disulfide reductase activity	6	1	Selenot	0.050333
0005332	Gamma-aminobutyric acid:sodium symporter activity	6	1	Slc6a6	0.050333
0004601	Peroxidase activity	44	2	Hba-a2, Hbb-bs	0.054596
0099635	Voltage-gated calcium channel activity involved in positive regulation of presynaptic cytosolic calcium levels	7	1	Cnr1	0.058473
0010385	Double-stranded methylated DNA binding	7	1	Egr1	0.058473
0030911	TPR domain binding	7	1	Hsp90aa1	0.058473
1905538	Polysome binding	7	1	Impact	0.058473
1904315	Transmitter-gated ion channel activity involved in regulation of postsynaptic membrane potential	47	2	Gabra2, Gabrb1	0.061369
0061797	pH-gated chloride channel activity	48	2	Gabra2, Gabrb1	0.063687
0030235	Nitric-oxide synthase regulator activity	8	1	Hsp90aa1	0.066545
0031995	Insulin-like growth factor II binding	8	1	Igfbp5	0.066545
0010997	Anaphase-promoting complex binding	8	1	Pten	0.066545
1990247	N6-methyladenosine-containing RNA binding	8	1	Ythdc1	0.066545
0008028	Monocarboxylic acid transmembrane transporter activity	52	2	Slc6a6, Slco1c1	0.073247
0031957	Very long-chain fatty acid-CoA ligase activity	9	1	Acsl4	0.074547
0030957	Tat protein binding	9	1	Dnaja1	0.074547
0034046	Poly(G) binding	9	1	Fmr1	0.074547
0003691	Double-stranded telomeric DNA binding	9	1	Pura	0.074547

GO term	Description	Detected Genes	DE Genes	DE Genes (Names)	P-values
0005544	Calcium-dependent phospholipid binding	53	2	Anxa5, Cpne7	0.075705
0035197	siRNA binding	10	1	Fmr1	0.082482
0045159	Myosin II binding	10	1	Gsn	0.082482
0043208	Glycosphingolipid binding	10	1	Mag	0.082482
0008199	Ferric iron binding	10	1	Trf	0.082482
0005388	Calcium-transporting ATPase activity	11	1	Anxa5	0.090349
0004143	Diacylglycerol kinase activity	11	1	Dgkb	0.090349
0016274	Protein-arginine N-methyltransferase activity	11	1	Fbxo11	0.090349
0008503	Benzodiazepine receptor activity	11	1	Gabra2	0.090349
0008429	Phosphatidylethanolamine binding	11	1	Pltp	0.090349
1901611	Phosphatidylglycerol binding	11	1	Pltp	0.090349
0005086	ARF guanyl-nucleotide exchange factor activity	11	1	Psd3	0.090349
1990459	Transferrin receptor binding	11	1	Trf	0.090349
0019829	Inorganic cation-transporting ATPase activity	59	2	Anxa5, mt-Atp6	0.09098
0042625	ATPase coupled ion transmembrane transporter activity	61	2	Anxa5, mt-Atp6	0.096257
0000900	Translation repressor activity, mRNA regulatory element binding	12	1	Pura	0.098149
0044548	S100 protein binding	12	1	S100a1	0.098149
0042910	Xenobiotic transporter activity	12	1	Slc6a6	0.098149

Table 4c

Subset of significantly affected gene ontology categories forming cellular components. Green, negative fold changes indicate downregulation. Red, positive fold changes indicate upregulation.

GO term	Description	Total Genes	DE Genes	DE Genes (Names)	P-values
0043218	Compact myelin	5	4	Mag, Mbp, Pllp, Pmp22	2.639E-07
0043209	Myelin sheath	182	12	Cldn11, Cnp, Dld, Gjc2, Gsn, Hsp90aa1, Hspa5, Mag, Mbp, Mog, Plcb1, Sucla2	2.427E-05
0035749	Myelin sheath adaxonal region	6	3	Cnp, Mag, Pten	6.830E-05
0000235	Astral microtubule	8	3	Dynlt3, Map9, Pafah1b1	1.869E-04
0098982	GABA-ergic synapse	104	8	Camk4, Cnr1, Gabra2, Gabrb1, Gabrd, Nrxn1, Plcb1, Slc6a6	1.951E-04
1990015	Ensheathing process	2	2	Mag, Myoc	2.329E-04
0097453	Mesaxon	2	2	Mag, Myoc	2.329E-04
0043197	Dendritic spine	181	10	Akap5, Arc, Fmr1, Fxr1, Homer1, Lpar1, Mob4, Pten, Slc8a1, Syndig1	4.823E-04
0043198	Dendritic shaft	69	6	Akap5, Hcn1, Homer1, Lpar1, Slc8a1, Syndig1	6.462E-04
0034663	Endoplasmic reticulum chaperone complex	12	3	Hsp90b1, Hspa5, Sdf2l1	7.018E-04
0042824	MHC class I peptide loading complex	14	3	B2m, H2-D1, H2-K1	1.135E-03
0005790	Smooth endoplasmic reticulum	31	4	Dnajc3, Fmr1, Hsp90b1, Hspa5	1.214E-03
0043220	Schmidt-Lanterman incisure	15	3	Mag, Myoc, Pten	1.403E-03
1902737	Dendritic filopodium	5	2	Fmr1, Fxr1	2.259E-03
0030139	Endocytic vesicle	154	8	Gsn, Kif5b, Lpar1, Nrxn1, Rab8b, Rab9b, Rabep1, Trf	2.573E-03
1990712	HFE-transferrin receptor complex	6	2	B2m, Trf	3.354E-03
0031415	NatA complex	6	2	Naa15, Naa50	3.354E-03
0001651	Dense fibrillar component	6	2	Ncl, Top1	3.354E-03
0042579	Microbody	127	7	Acbd5, Acsl4, Crot, Idi1, Pex13, Pnpla8, Rab8b	3.400E-03
0030670	Phagocytic vesicle membrane	21	3	B2m, H2-D1, H2-K1	3.832E-03
0005797	Golgi medial cisterna	23	3	H2-D1, H2-K1, Yipf6	4.990E-03
0060076	Excitatory synapse	46	4	Akap5, Homer1, Neto1, Syndig1	5.266E-03
0060077	Inhibitory synapse	24	3	Gabra2, Gad2, Nrxn1	5.639E-03
0005844	Polysome	47	4	Fmr1, Fxr1, Impact, Upf2	5.688E-03
0030666	Endocytic vesicle membrane	26	3	B2m, H2-D1, H2-K1	7.083E-03
0099524	Postsynaptic cytosol	26	3	Fmr1, Homer1, Pten	7.083E-03

GO term	Description	Total Genes	DE Genes	DE Genes (Names)	P-values
0005876	Spindle microtubule	51	4	Bod1l, Dynlt3, Map9, Pafah1b1	7.600E-03
0035748	Myelin sheath abaxonal region	9	2	Cnp, Myoc	7.809E-03
0044326	Dendritic spine neck	9	2	Fmr1, Fxr1	7.809E-03
0005833	Hemoglobin complex	9	2	Hba-a2, Hbb-bs	7.809E-03
0051286	Cell tip	10	2	Rab8b, Trf	9.663E-03
0005777	Peroxisome	119	6	Acbd5, Acsl4, Crot, Idi1, Pex13, Pnpla8	9.958E-03
0098845	Postsynaptic endosome	12	2	Akap5, Arc	0.0139
0009898	Cytoplasmic side of plasma membrane	61	4	Akap5, G6pdx, Litaf, Pten	0.0141
1990707	Nuclear subtelomeric heterochromatin	1	1	Atrx	0.0153
0030990	Intraciliary transport particle	1	1	Dync2li1	0.0153
0005969	Serine-pyruvate aminotransferase complex	1	1	Eea1	0.0153
0071540	Eukaryotic translation initiation factor 3 complex, eIF3e	1	1	Eif3a	0.0153
0016028	Rhabdomere	1	1	Mertk	0.0153
0034678	Integrin alpha8-beta1 complex	1	1	Npnt	0.0153
0005943	Phosphatidylinositol 3-kinase complex, class IA	1	1	Pik3ca	0.0153
0045239	Tricarboxylic acid cycle enzyme complex	13	2	Dld, Sucla2	0.0163
1902711	GABA-A receptor complex	13	2	Gabra2, Gabrb1	0.0163
0071556	Integral component of lumenal side of endoplasmic reticulum membrane	13	2	H2-D1, H2-K1	0.0163
1990124	Messenger ribonucleoprotein complex	14	2	Fmr1, Hnrnpa3	0.0188
0005778	Peroxisomal membrane	38	3	Pex13, Pnpla8, Rab8b	0.0201
0032590	Dendrite membrane	39	3	Akap5, Gabra2, Hcn1	0.0215
0098839	Postsynaptic density membrane	39	3	Arc, Neto1, Syndig1	0.0215
0099522	Region of cytosol	40	3	Fmr1, Homer1, Pten	0.0230
0005753	Mitochondrial proton-transporting ATP synthase complex	16	2	mt-Atp6, mt-Atp8	0.0243
0099634	Postsynaptic specialization membrane	41	3	Arc, Neto1, Syndig1	0.0246
0045178	Basal part of cell	17	2	Cldn11, Trf	0.0272
0033270	Paranode region of axon	17	2	Gjc2, Mag	0.0272
0055037	Recycling endosome	113	5	Akap5, Avl9, Eea1, Mctp1, Trf	0.0298
0032433	Filopodium tip	18	2	Fmr1, Fzd3	0.0303
0030140	Trans-Golgi network transport vesicle	18	2	Gopc, Rab8b	0.0303
0072563	Endothelial microparticle	2	1	Anxa5	0.0303

GO term	Description	Total Genes	DE Genes	DE Genes (Names)	P-values
0043614	Multi-eIF complex	2	1	Eif3a	0.0303
0032998	Fc-epsilon receptor I complex	2	1	Fcer1g	0.0303
0061202	Clathrin-sculpted gamma-aminobutyric acid transport vesicle membrane	2	1	Gad2	0.0303
0097226	Sperm mitochondrial sheath	2	1	Hsp90aa1	0.0303
0098560	Cytoplasmic side of late endosome membrane	2	1	Litaf	0.0303
0005818	Aster	2	1	Map9	0.0303
1904423	Dehydrodolichyl diphosphate synthase complex	2	1	Nus1	0.0303
0030426	Growth cone	197	7	Cnr1, Fmr1, Fxr1, Hsp90aa1, Kif5b, Nrxn1, Pafah1b1	0.0321
0044449	Contractile fiber part	198	7	Anxa5, Fxr1, Homer1, Jph1, Npnt, S100a1, Slc8a1	0.0328
0044295	Axonal growth cone	46	3	Hsp90aa1, Kif5b, Nrxn1	0.0331
0090723	Growth cone part	19	2	Fmr1, Pafah1b1	0.0336
0043034	Costamere	19	2	Fxr1, Homer1	0.0336
0005922	Connexin complex	19	2	Gjb1, Gjc2	0.0336
0043679	Axon terminus	121	5	Anxa5, Chrm3, Fmr1, Hcn1, Slc8a1	0.0383
0045335	Phagocytic vesicle	83	4	Gsn, Kif5b, Rab8b, Rab9b	0.0384
0030018	Z disc	124	5	Anxa5, Homer1, Jph1, S100a1, Slc8a1	0.0418
0099055	Integral component of postsynaptic membrane	167	6	Chrm3, Gabra2, Gabrd, Neto1, Slc6a6, Slc8a1	0.0435
0005921	Gap junction	22	2	Gjb1, Gjc2	0.0440
0098855	HCN channel complex	3	1	Hcn1	0.0452
0097524	Sperm plasma membrane	3	1	Hsp90aa1	0.0452
0014701	Junctional sarcoplasmic reticulum membrane	3	1	Jph1	0.0452
0098559	Cytoplasmic side of early endosome membrane	3	1	Litaf	0.0452
0034457	Mpp10 complex	3	1	Mphosph10	0.0452
1990415	Pex17p-Pex14p docking complex	3	1	Pex13	0.0452
0042709	Succinate-CoA ligase complex	3	1	Sucla2	0.0452
0035327	Transcriptionally active chromatin	23	2	Aff4, Psip1	0.0477
0031307	Integral component of mitochondrial outer membrane	24	2	Armcx3, Gdap1	0.0515
0032279	Asymmetric synapse	25	2	Akap5, Chrm3	0.0555
0005868	Cytoplasmic dynein complex	25	2	Dync2li1, Dynlt3	0.0555
0032783	ELL-EAF complex	4	1	Aff4	0.0598
0043159	Acrosomal matrix	4	1	Dld	0.0598

GO term	Description	Total Genes	DE Genes	DE Genes (Names)	P-values
0044308	Axonal spine	4	1	Eea1	0.0598
1990812	Growth cone filopodium	4	1	Fmr1	0.0598
0097444	Spine apparatus	4	1	Fmr1	0.0598
0019034	Viral replication complex	4	1	Fmr1	0.0598
0030478	Actin cap	4	1	Gsn	0.0598
0042567	Insulin-like growth factor ternary complex	4	1	Igfbp5	0.0598
0035976	Transcription factor AP-1 complex	4	1	Junb	0.0598
0098574	Cytoplasmic side of lysosomal membrane	4	1	Litaf	0.0598
0033269	Internode region of axon	4	1	Mbp	0.0598
0031021	Interphase microtubule organizing center	4	1	Mzt1	0.0598
0030289	Protein phosphatase 4 complex	4	1	Ppp4r2	0.0598
0008305	Integrin complex	28	2	Npnt, Pmp22	0.0679
0098563	Intrinsic component of synaptic vesicle membrane	63	3	Gabra2, Rab3c, Wfs1	0.0719
0070971	Endoplasmic reticulum exit site	29	2	H2-D1, H2-K1	0.0722
0031256	Leading edge membrane	146	5	Akap5, Gabra2, Hcn1, Hsp90aa1, Psd3	0.0737
0061673	Mitotic spindle astral microtubule	5	1	Dynlt3	0.0741
0044094	Host cell nuclear part	5	1	Fmr1	0.0741
1990769	Proximal neuron projection	5	1	Gjc2	0.0741
0030485	Smooth muscle contractile fiber	5	1	Npnt	0.0741
0016586	RSC complex	5	1	Pbrm1	0.0741
0034991	Nuclear meiotic cohesin complex	5	1	Smc3	0.0741
0097433	Dense body	5	1	Trf	0.0741
0098984	Neuron to neuron synapse	30	2	Akap5, Chrm3	0.0766
0030672	Synaptic vesicle membrane	66	3	Gad2, Mctp1, Syndig1	0.0802
0005791	Rough endoplasmic reticulum	67	3	Ccdc47, Clock, Fmr1	0.0830
0005726	Perichromatin fibrils	6	1	Clock	0.0883
0031466	Cul5-RING ubiquitin ligase complex	6	1	Cul5	0.0883
0071598	Neuronal ribonucleoprotein granule	6	1	Fmr1	0.0883
0008274	Gamma-tubulin ring complex	6	1	Mzt1	0.0883
0090724	Central region of growth cone	6	1	Pafah1b1	0.0883
0000932	Cytoplasmic mRNA processing body	72	3	Dcp2, Pnrc2, Top1	0.0979

GO term	Description	Total Genes	DE Genes	DE Genes (Names)	P-values
0032040	Small-subunit processome	35	2	Krr1, Mphosph10	0.0997